Available online at www.sciencedirect.com
ScienceDirect
Renewable and Sustainable Energy Reviews 13 (2009) 1–39
RENEWABLE & SUSTAINABLE ENERGY REVIEWS
www.elsevier.com/locate/rser

Condition monitoring and fault detection of wind turbines and related algorithms: A review

Z. Hameed[a], Y.S. Hong[a], Y.M. Cho[a], S.H. Ahn[b,*], C.K. Song[c]

[a]School of Mechanical and Aerospace Engineering, Building 301, Room 1402, Seoul National University, San 56-1 Shinlim-dong, Kwanak-ku, Seoul 151-744, Republic of Korea
[b]School of Mechanical and Aerospace Engineering & Institute of Advanced Machinery and Design, Seoul National University, Shinlim-Dong San 56-1, Seoul 151-742, Republic of Korea
[c]School of Mechanical and Aerospace Engineering, Gyeongsang National University, Jinju, Gyeongnam 660-701, Republic of Korea

Received 16 April 2007; accepted 30 May 2007

Abstract

Renewable energy sources like wind energy are copiously available without any limitation. Wind turbines are used to tap the potential of wind energy, which is available in millions of MW. Reliability of wind turbine is critical to extract this maximum amount of energy from the wind. We reviewed different techniques, methodologies and algorithms developed to monitor the performance of wind turbine as well as for an early fault detection to keep away the wind turbines from catastrophic conditions due to sudden breakdowns. To keep the wind turbine in operation, implementation of condition monitoring system (CMS) and fault detection system (FDS) is paramount and for this purpose ample knowledge of these two types of systems is mandatory. So, an attempt has been made in this direction to review maximum approaches related to CMS and FDS in this piece of writing.

Keywords: CMS; FDS; WEC; Reliability; Algorithm

Contents

Abbreviations: WEC, wind energy converter; HMS, health-monitoring system; FFT, fast Fourier transform; DTSS, distributed temperature and strain sensor; FO, fibre optic; FBG, fibre Bragg grating; SPU, signal-processing unit; CCD, charge-coupled device; GFRP, glass fibre-reinforced plastics; OCT, optical coherence tomography; NIST, National Institute of Standards and Technology; AE, acoustic emission; SPR, supervised pattern recognition; UPR, unsupervised pattern recognition; PR, pattern recognition; AEL, acoustic emission loading; SNS, structural neural systems; PZT, lead zirconate titanate; PDS, power density spectrum; DFIG, doubly fed induction generator; AI, artificial intelligence; ARRs, address range registers; DOF, degree of freedom; SLDV, scanning laser doppler vibrometer; FRF, frequency response function; TF, transmittance function; ODS, operational deflection shape; MTS, material testing system; TE, thermoelastic; TSA, thermoelastic stress analysis; SPATE, stress pattern analysis by thermal emission; SIMAP, intelligent system for predictive maintenance; TV, torsional vibration; MCSA, machine current signature analysis; SET, Institute fur Solare Energieveersorgungstechnik; SKF, Svenska Kullagerfabriken

*Corresponding author. Tel.: +82 2 880 7110; fax: +82 2 883 0179.
E-mail address: ahnsh@snu.ac.kr (S.H. Ahn).

1364-0321/$ - see front matter
doi:10.1016/j.rser.2007.05.008

1. Introduction

The wind turbine technology has a unique technical identity and unique demands in terms of the methods used for design. Remarkable advances in the wind power design have been achieved due to modern technological developments. Since 1980, advances in aerodynamics, structural dynamics and "micrometeorology" have contributed to a 5% annual increase in the energy yield of the turbines. Current research techniques are producing stronger, lighter and more efficient blades for the turbines. The annual energy output for turbine has increased enormously and the weights of the turbine and the noise they emit have been halved over the last few years. We can generate more power from wind energy by establishment of more number of wind monitoring stations, selection of wind farm site with suitable wind electric generator, improved maintenance procedure of wind turbine to increase the machine availability, use of high-capacity machine, low-wind regime turbine, higher tower height, wider swept area of the rotor blade, better aerodynamic and structural design, faster computer-based machining technique, increasing power factor and better policies from government [1].

Even among other applications of renewable energy technologies, power generation through wind has an edge because of its technological maturity, good infrastructure and relative cost competitiveness. Wind energy is expected to play an increasingly important role in the future national energy scene [2,3]. Wind turbines convert the kinetic energy of the wind to electrical energy by rotating the blades. Greenpeace states that about 10% electricity can be supplied by the wind by the year 2020. At good windy sites, it is already competitive with that of traditional fossil fuel generation technologies. With this improved technology and superior economics, experts predict wind power would capture 5% of the world energy market by the year 2020. Advanced wind turbine must be more efficient, more robust and less costly than current turbines [1].

Reliability of any design is the most important feature and this can be ensured by overwhelming the previous weaknesses and faults occurred in the design and then formulating novel strategies and techniques to minimize these shortcomings. By doing so, the reliability and robustness of that design can be enhanced. One means of achieving this level is to devise and implement efficient, adaptable and responsive systems of condition monitoring and fault detection systems (FDSs) especially on rotational structures of the wind energy converter (WEC).

Condition monitoring system (CMS) (HMS—health-monitoring system) plays a pivotal role in establishing a condition-based maintenance and repair (M&R), which can be more beneficial than corrective and preventive maintenance. To achieve this objective, there is a need to develop an efficient fault prediction algorithm and this algorithm shall be the basis of CMS. Autonomous online CMSs with integrated fault detection algorithms allow early warnings of mechanical and electrical defects to prevent major component failures. Side effects on other components can be reduced significantly. Many faults can be detected while the defective component is still operational. Thus necessary repair actions can be planned in time and need not be taken immediately and this fact is of special importance for off-shore plants where bad conditions (storm, high tide, etc.) can prevent any repair actions

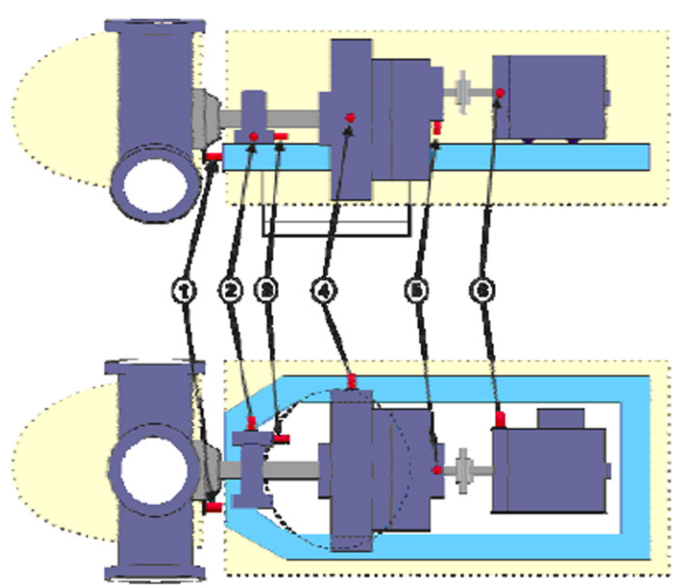


Fig. 1. Condition monitoring sensor configuration for horizontal axis wind energy converters.

Table 1
Function of sensors in CMS [4]

Label number of sensor	Description
1	Measure absolute position of rotor to perform phase sensitive narrow band analysis (special FFT-algorithm for signal processing)
2, 3, and 4	Measure the nacelle oscillation induced by rotational speed of the rotor with static accelerometers (with lower cutoff frequency of 0 Hz
5 and 6	Measure the vibration induced by bearings and gearwheels at a frequency range from 1 to 20,000 Hz

for several weeks [4]. Fig. 1 shows the architectures of CMS along with sensor description in Table 1.

FDS have been successfully applied in many kinds of technical processes to improve operation reliability and safety. For example, in the supervision of power station turbines and aircraft engines vibration monitoring is state of the art. Advanced fault detection techniques have recently been applied to machine tools, e.g., cutting tools in turning, industrial robots, automotive power trains and paper machines [5,6].

FDSs evaluate measured process data (e.g., using spectral analysis for vibration monitoring) to isolate incipient faults at a very early stage that is before they become optically or acoustically manifest. This way, a plant can often be repaired before the faulty component actually fails and, possibly, causes damage to other parts of the plant. Obviously, these issues are a major concern in wind energy technology, too, especially for the development of large-scale WECs [7].

Implementation of FDS entails benefits of good operational safety due to its main features of early warning system and cost effectiveness because condition-based maintenance is carried out in spite of corrective or preventive maintenances. Initial investment is needed to develop and implement the FDS but the continuous production of power without any breakdown offsets this investment cost substantially. Offshore wind farms extract more benefits of this system due to their farthest and remote locations where huge costs have to be paid to move the logistics than onshore wind farms. The countries which have poor lifting and handling equipments like cranes, fork lifts, etc., and they are interested to get power through WEC, then they must install FDS to obtain feasible power rates by avoiding the frequency of sudden breakdowns and associated huge maintenance and logistic costs.

Failure statistics of WECs from the "Scientific Measurement and Evaluation Program" (WMEP) in the German "250 MW"—field test have shown that in 1992 and 1993 about 25% of a total number of 5500 repair actions were caused by loose components, wear and failure [8]. Since the replacement of main components of a WEC is a difficult and very costly affair, improved maintenance procedures can lead to essential cost reductions. Therefore, an FDS for WECs may offer a number of benefits [7]:

(i) *Avoidance of premature breakdown*: The most important aspect of incipient fault detection is to prevent catastrophic failures and secondary defects. For example, late detection of a rotor-bearing fault may in the worst case imply complete destruction of the WEC.
(ii) *Reduction of maintenance costs*: With on-line monitoring, inspection intervals can be increased. Replacement of intact parts is avoided by condition-based maintenance.
(iii) *Supervision at remote sites, remote diagnosis*: Large wind turbines are usually built at remote sites where, in contrast to industrial machinery, optical or acoustical changes may not be observed for a quite long time. On-line monitoring systems can detect such changes at an early stage and, if equipped with a modem, send a warning and diagnostic details to the maintenance staff.
(iv) *Improvement of the capacity factor*: With early warning of impending failures, repair actions need not be taken immediately. They can be carried out in a period of low wind speed when the WEC is off-line that is without affecting capacity factor.
(v) *Support for further development of a WEC*: An FDS yields detailed information on the dynamic behavior of a wind turbine over long periods of time that may help optimizing the WEC design.

ISET is currently developing a FDS for WECs in cooperation with Carl Schenck AG, Darmstadt (Germany). An overview of the main components to be monitored and some possible faults are shown in Fig. 2. Faults like imbalance, wear, fatigue and impending cracks in rotor blades, bearings, shafts, in the gearbox, the generator and in the yaw- and the pitch angle mechanism are in the scope of the FDS development [7].

The online monitoring and fault detection concepts are relatively new in WEC arena and are flourishing on a rapid scale. Novel and innovative ways are being developed to monitor the performance of the system accurately and then collecting the operational data to verify the design values and on the basis of this data, further improvements are suggested/carried out for future designs. An early knowledge of impending faults like initiation of crack, wear, etc. and failure like rotor mass imbalance, abnormal sound from main bearing, etc. is revealing the degree of reliability of that system. A more responsive system toward any abnormality occurring in the WEC is indicating that the system is more reliable and robust. To achieve all these goals, certain methodologies and techniques have to be developed for making an existing or future system more reliable and robust than their predecessors. One solution to this problem is to build the algorithms on the basis of

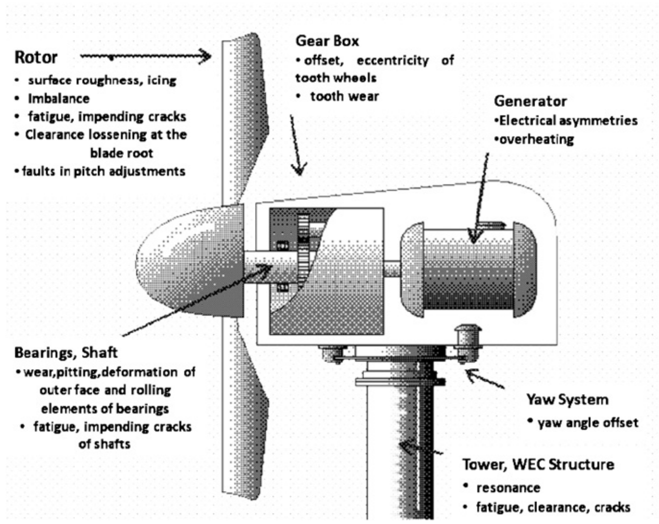


Fig. 2. Faults in a WEC.

prescribed performance parameters, incorporating in these algorithms all the likelihood causes of detection and failure, and then devising an intelligent and reliable alarming system for an accurate interpretation of these alarms and subsequently taking necessary preventive or corrective actions.

2. CMS, methodology and algorithms

2.1. CMS

CMS is a tool for telling in what condition the components in a system are. CMS is being used today in many other applications, but in the wind power industry it is relatively new. With CMS, a prediction of impending failure is given for each component, and therefore M&Rs can then be better scheduled. The CMS for the g2earbox primarily measures vibrations, but a supervision of the oil is also necessary. The CMS used today are capable of detecting failures, well in time prior to a failure and they are even able to predict which component inside the gearbox is defective [9].

Consider that a modern wind turbine operates for about 13 years in a design life of 20 and is almost always unattended. A motor vehicle, by comparison, is manned, frequently maintained and its design life of about 150,000 km is equivalent to just 4 months of continuous operation. The wind turbine is in several ways a unique power generating system as the power train components are subject to highly irregular loading from turbulent wind conditions, and the number of fatigue cycles experienced by the major structural components can be far greater than for other rotating machines [10].

A report from Elforsk shows that in recent years the amount of damage claims has increased according to a report from a German insurance company. It is suggested that the reasons for this development are given in Table 2 [12].

Table 2
Causes of damage claims

Technical reasons	Operation and maintenance reasons
Insufficient prototype testing	Bad documentation
Excessively fast development	Lack of appropriate maintenance
Insufficient dimensioning and wrong selection of components	Lack of quality control
–	Insufficient stocking of spare parts

While studying the main reasons of damages, it is evident to incorporate a monitoring device, which shall be able to overcome the shortcomings during prototyping testing, development phase, and inappropriate maintenance strategies. The rotational components are working under dynamic loads and so they are more susceptible to failures, so there is an utmost need to develop monitoring techniques for an early warning of the failure and any other kind of impending danger. The failure is unavoidable but losses due to sudden faults and damages can be minimized by installing early monitoring systems to warn any looming catastrophe. By doing this, production losses will be minimized and this will contribute in making our existing system more efficient and reliable.

WEC is not the only beneficiary of CMS and there are also other industries, which are equipped with this kind of monitoring system, e.g., pulp industry. In 2001, a project for examining the possibility of using a CMS was undertaken by Elforsk in cooperation with Göteborgs Energi and SKF Nova. At that time no monitoring system was available for a wind turbine and SKF Nova developed a system that was tested on a Vestas V44 turbine [13].

By doing an in depth study of the failures one can find out which components fail, how often they fail and if it is possible to measure the wear of the component and from this measurement decide when to perform the maintenance. The wind power systems usually have a high rate of availability, but this is because of frequent maintenance [14]. The need arises to minimize the frequency of maintenance to enhance the reliability of system with minimum number of faults, damages, downtimes, and smaller duration of repairs.

Before going on towards studying the main components of CMS, here some characteristics of monitoring systems are listed in Table 3, which reveals the importance of monitoring system.

2.2. Methodology

The area of CMS can be viewed as two separate fields of technology. On one hand as sensor technology and on the other hand as a diagnostic and condition monitoring technology [15]. So for designing an expert system of CMS, ample knowledge is required of sensors, their

Table 3
Characteristics of condition monitoring systems [13]

Characteristics	Advantages	Benefits
Early warning	• Avoid breakdowns • Better planning of maintenance	• Avoid repair costs • Minimize downtime
Identification of problem	• Right service at the right time • Minimizing unnecessary replacements. • Problems resolved before the time of guarantee expires	• Prolonged lifetime • Lowered maintenance costs • Quality-controlled operations during time of guarantee
Continuous monitoring	• Constant information that the wind power system is working	• Security. Less stress

characteristics, performance and reliability. The reliable data acquisition regarding the impending failure or damage of certain components can only be acquired by optimally placing the sensors at their appropriate place. Placement of sensor is paramount in extracting trustworthy data from the operating system. The diagnostic and condition monitoring technology is related to first diagnose the criticality of each component on the operation of WEC, and then on the basis of this analysis, proper description of the parameters of those component/components which could lead to failure .The primary deciding factor should be to devise monitoring system for those components which cause more down time if their breakdown occurs like gearbox, main bearings of generator, etc.

2.2.1. Basis of CMS techniques

The CMS techniques, on the basis of which monitoring system of whole WEC or selected components of it can be established, are summarized below along with brief description [16,17].

(i) *Vibration analysis*: Vibration analysis is the most known technology applied for condition monitoring, especially for rotating equipment. The types of sensors used depend more or less on the frequency range, relevant for the monitoring:
- position transducers for the low-frequency range
- velocity sensors in the middle frequency area
- accelerometers in the high-frequency range
- and spectral emitted energy (SEE) sensors for very high frequencies (acoustic vibrations).

For wind turbines this type of monitoring is applicable for monitoring the wheels and bearings of the gearbox, bearings of the generator and the main bearing.

Signal analysis requires specialized knowledge. Suppliers of the system offer mostly complete systems, which include signal analysis and diagnostics. The monitoring itself is also often executed by specialized suppliers who also perform the maintenance of the components. The costs are compensated by reduction of production losses. Application of vibration monitoring techniques and working methods for wind turbines differ from other applications with respect to:
- *The dynamic load characteristics and low rotational speeds*: In other applications, loads and speed are often constant during longer periods, which simplify the signal analysis. For more dynamic applications, like wind turbines, the experience is very limited.
- *The high investment costs in relation to costs of production losses*: The investments in conditions monitoring equipment is normally covered by reduced production losses. For wind turbines, especially for land applications, the production losses are relatively low. So the investment costs should for a important part be paid back by reduction of maintenance cost and reduced costs of increased damage.

(ii) *Oil analysis*: Oil analysis may have two purposes:
- safeguarding the oil quality (contamination by parts, moist)
- safeguarding the components involved (characterization of parts).

Oil analysis is mostly executed off line, by taking samples. However for safeguarding the oil quality, application of on-line sensors is increasing. Sensors are nowadays available, at an acceptable price level for part counting and moist. Besides this, safeguarding the state of the oil filter (pressure loss over the filter) is mostly applied nowadays for hydraulic as well as for lubrication oil. Characterization of parts is often only performed in case of abnormalities. In case of excessive filter pollution, oil contamination or change in component characteristic, characterization of parts can give an indication of components with excessive wear.

(iii) *Thermography*: Thermograhy is often applied for monitoring and failure identification of electronic and electric components. Hot spots, due to degeneration of components or bad contact can be identified in a simple and fast manner.

(iv) *Physical conditions of materials*: This type of monitoring is mainly focused on crack detection and growth. Methods are normally off line and not suitable for on-line condition monitoring of wind turbines. Exception might be the usage of optical fuses in the blades and acoustic monitoring of structures.

(v) *Strain measurements*: Strain measurement by strain gauges is a common technique, however not often applied for condition monitoring. Strain gauges are not robust on a long term. Especially for wind turbines, strain measurement can be very useful for lifetime prediction and safeguarding of the stress level, especially for the blades. More robust sensors might open an interesting application area.

Optical fibre sensors are promising, however still too expensive and not yet state-of-the-art. Availability of cost effective systems, based on fibre optics (FO) can be expected within some years. Strain measurement as condition monitoring input will then be of growing importance.

(vi) *Acoustic monitoring*: Acoustic monitoring has a strong relationship with vibration monitoring. However there is also a principle difference. While vibration sensors are rigid mounted on the component involved, and register the local motion, the acoustic sensors "listen" to the component. They are attached to the component by flexible glue with low attenuation. These sensors are successfully applied for monitoring bearing and gearboxes.

There are two types of acoustic monitoring. One method is the passive type, where the excitation is performed by the component itself. In the second type, the excitation is externally applied.

(vii) *Electrical effects*: For monitoring electrical machines, MCSA is used to detect unusual phenomena. For accumulators the impedance can be measured to establish the condition and capacity.

For medium and high voltage grids, a number of techniques are available

- discharge measurements
- velocity measurements for switches
- contact force measurements for switches
- oil analysis for transformers.

For cabling, isolation faults can be detected. These types of inspection measurements do not directly influence the operation of the wind turbines.

(viii) *Process parameters*: For wind turbines, safeguarding based on process parameters is of course common practice. The control systems become more sophisticated and the diagnostic capabilities improve. However safeguarding is still largely based on level detection or comparison of signals, which directly result in an alarm when the signals become beyond predefined limit values. At present, more intelligent usage of the signals based on parameter estimation and trending is not common practice in wind turbines.

(ix) *Performance monitoring*: The performance of the wind turbine is often used implicitly in a primitive form. For safeguarding purposes, the relationship between power, wind velocity, rotor speed and blade angle can be used and in case of large deviations, an alarm is generated. The detection margins are large in order to prevent for false alarms. Similar to estimation of process parameter, more sophisticated methods, including trending, are not often used.

2.2.2. Important issues before CMS implementation

Before condition monitoring can be applied successfully for wind energy, at least the following items should be solved [17]:

(i) *Improvement of safeguarding functions*: Wind turbine control systems incorporate an increasing functionality. Some of the functions come very close to condition monitoring. With relatively low costs, some more intelligence can be added, which makes early fault detection based on trend analysis possible (pitch mechanism, brake, yaw system and generator).

(ii) *Development of global techniques*: Apart from safeguarding, trending of wind turbine main parameters (power, pitch angle, rotational speed, wind velocity and yaw angle) can give global insight in the operation in the turbine. It may be possible to detect that "something might be wrong". Dirt on the blades has a strong reducing effect on the power production, which can also be detected by trend analysis.

(iii) *Adaptation of existing systems*: In other industries, condition-monitoring provisions are normally separate systems, apart from the machine control and safe guarding functions. The monitoring is often focused on a very limited number of aspects. For wind turbines however, the system to be monitored is rather complex and the margins for investments are small. The number of systems is very high. So when existing systems are used, the adaptation should not only be focused on the dynamic load behavior, but also on streamlining the system and integration.

(iv) *Information mapping*: Offshore wind turbines normally operate in a park, which is remote controlled from a central control room. Because a great number of turbines are controlled from the central facility, information should be processed and filtered before being reported to the operator and maintenance planning.

When applying condition-monitoring techniques in wind turbines, the following two pitfalls should be considered.

(a) *Application of existing techniques*: Only adaptation of existing systems is often not sufficient to make them suitable for wind turbines. Although the systems will "function" of course, the effectiveness can only be determined on the long term.

(b) *Robustness of secondary systems*: Manufacturers often have an aversion to a large amount of sensors. Failure of condition monitoring functions may never result in turbine stop. Operational decisions are made by the control system or by the operator.

2.3. Algorithms

The development and then applying algorithms is one way to establish an efficient and reliable operational and repair (O&R) system. These algorithms are developed and then implemented by keeping in view the main characteristics of the WEC, previous failure data, identifying components which will cause more downtime, components which are more prone to the initiation of crack, wear, misalignment, etc. More emphasis will be focused on the rotational components and the structures, which are directly supporting those rotations like the bearing, which is supporting the generator shaft.

The implementation of CMS depends upon certain parameters, which are to be selected by the user itself or to be obtained from the manufacturer because thorough understanding of all performance parameters is paramount. Every manufacture of WEC uses different approaches in designing, developing and manufacturing it, so the performance parameters shall be selected keeping in view all these aspects. One example is listed below in Table 4 in which CMS parameters of two manufacturers of WEC are compared. There are some parameters, which are common, and some ones, which are not in common.

It is quite important to choose which components will be monitored by CMS and then most important thing is to select which parameters will be monitored to sense any abnormality and then initiation of warning signal. For selecting the parameters, the manufacturer's recommendations should be given proper importance. Now a day, manufactures also started to prepare WEC with embedded CMS.

Table 4
Comparison of CMS parameters of two manufactures of WEC [17]

	LAGERWEY 50/750	ENRON 1,5S(Siemens)
Performance measurements of pitch system		
Pitch angle (3)	●	●
Desired pitch angle (1)	×	●
Current to servomotor (3)	●	●
Pitch angle velocity (3)	●	×
Pitch angle set point (1)	●	×
Servo speed set point (3)	●	×
Temperature reduction box (3)	●	●
Temperature servo motor (3)	●	×
Status signal servo brake	●	×
Status emergency	●	×
Accumulator current	●	×
Motor current	×	●
Measurement of main bearing		
Acceleration main bearing (transversal)	×	●
Acceleration main bearing (radial)	×	●
Main bearing temperature	●	●
Vibration	●	×
General measurements of the turbine		
Wind speed	×	●
Rotor speed	●	●
Azimuth angle	●	●
0Electrical power	●	●
Wind speed met mast	●	×
Wind speed wind turbine	●	×
Wind direction met mast	●	×
Yaw angle	×	●
Yaw misalignment	●	●
Air temperature	●	●
Air pressure	●	●
Rain detection	●	●
Unbalance	×	●
Main shaft torque	×	●
Lead lag moment blade root	×	●
Flap moment blade root	×	●
Measurement of gearbox and generator parameters		
Acceleration gearbox (transversal)	×	●
Acceleration gearbox (radial)	×	●
Acceleration generator (radial)	×	●

2.3.1. Global CMSs

Apart from the applied condition monitoring techniques on subsystem level (gearbox, pitch mechanism, etc.) there is already a lot of information available in the wind turbine. Normally this information is only used at the level of safeguarding. Exceeding of the alarm levels often simply results in a wind turbine shut down and waiting for remote restart or repair. By application of more advanced methods of signal analysis, focused on trends of representative signals or combination of signals, significant changes in turbine behavior can be detected at an early stage. Because this approach is based on general turbine parameters, the information will also be of a global nature; so specific diagnostics cannot be expected [17].

This approach is cost effective as no additional investment is required in hardware but development of appropriate algorithm is mandatory to accomplish the task of monitoring the turbine as a whole. Data acquisition is necessary to study the malfunctions and other abnormalities, which occurred during the operation of turbine. Selection of monitoring variables is vital and utmost care has to be taken into this account. The parameters, which are responsible for long downtime in case of failures, should be given top most priority and this principle should be adopted in selecting all other monitoring parameters.

To develop a general-purpose algorithm for a whole turbine, strenuous efforts are needed in this arena. Main reasons are: (1) whole system becomes complicated when to define relationships among subsystems, components and subassemblies, (2) this approach is not fully matured and lot of time has to be spent to get some optimal or near optimal results.

2.3.1.1. Power engineering-based algorithm [18]. In this approach, it is easy to develop a wind turbine model in the electronics laboratory by substituting the wind turbine components with analogous to electronics parts.

Grid-connected windmill model is built in the laboratory as shown in Fig. 3. Windmill is replaced by a 2 kW thyristor-driven DC, torque controlled motor and torque of which is manually controlled. Mechanical braking is represented by switching off DC motor. A 2 kW induction generator is connected to windmill and terminal of generator are connected to 3-phase 400 V power grids. Rotational speed of motor shaft, the currents in the 3-phase to the generator and active power produced/consumed by the generator are being measured by this system.

Microprocessor kit (based on industrial 8-bit, 12 M Hz 80537-microcontroller which includes on-chip 12-channel 8-bit AD-converter, several 8-bit input/output ports and 2 serial communication channels is constructed to monitor and control the windmill model. Two electronics relays are used to operate the circuit breaker and start or stop the DC motor respectively. Special signal conditioning circuits have to be designed for the AD-converter to measure voltage range 0–5 V and to protect it from over/under voltage levels. With the interface, windmill can be fully monitored and controlled from the 80537-kit. Special programs are written in C on PC for microcontroller, and Visual Basic is used for PC programming. The operator maneuvers the windmill from the PC and windmill measurements are presented on the PC screen.

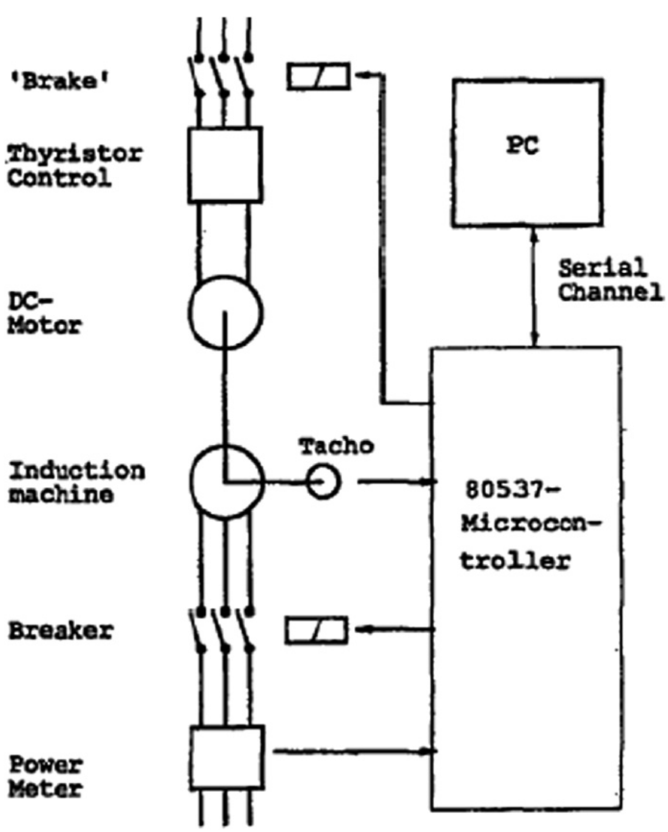


Fig. 3. Laboratory Model of Windmill.

Special algorithm can be developed after thorough understanding of the model to apprehend the monitoring procedure and this model is good for acquainting and training the students and operators about the monitoring of wind mill in the laboratory.

2.3.1.2. On-line contamination monitoring [19]. On-line contamination monitoring technology takes several forms. One system type applies a magnetic field to a contained fluid stream to detect the presence of ferro-magnetic debris, which is indicative of wear particles from rolling or rubbing contacts. Another type was originally developed for evaluating the cleanliness of fluids used in process industries, and has recently been adapted to hydraulic and lubricant fluids. These systems use a laser light source and target arrangement to count the particles, seen as obstructions, in a fluid stream. The more sophisticated systems can detect particle size and quantity and convert these into a standard metric for cleanliness, such as the ISO 4406 contamination code. A third system passes fluid over a fine mesh screen and detects the pressure drop as an indicator of accumulated contamination.

These techniques can be applied to monitor the whole WEC system as the debris, cleanliness and passages of fluid are involved approximately in all portions of WEC. So, by employing them singularly or combining them together give a good basis to first understand the behavior of fluid and formation debris and then developing the appropriate algorithm for monitoring of wind turbine as a whole.

2.3.2. CMS of subsystems

CMS, based on subsystems (or components), has progressed rapidly and has gained momentum. A number of researches are being carried out in this field and novel ideas are emanating which are making WECs popular and viable source of power. The implementation of CMS approach has enhanced the reliability and has increased the production of power by offsetting the initial cost being spent on its installation.

An overview of algorithms and analysis, which are developed to monitor the subsystem (components), is presented below.

2.3.2.1. Rotor. Rotor is a very critical component of WEC and a number of researches have been carried out to develop techniques pertaining to its health monitoring to reveal some hint about impending failure. The information about looming failure is precious and gives ample time to plan maintenance schedule and arrange necessary logistics.

Some of the approaches, which are directly related to condition monitoring of rotor, are summarized below.

Monitoring of power characteristic [20]: The relation between wind speed and active power output of a WEC provide information about the overall rotor condition.

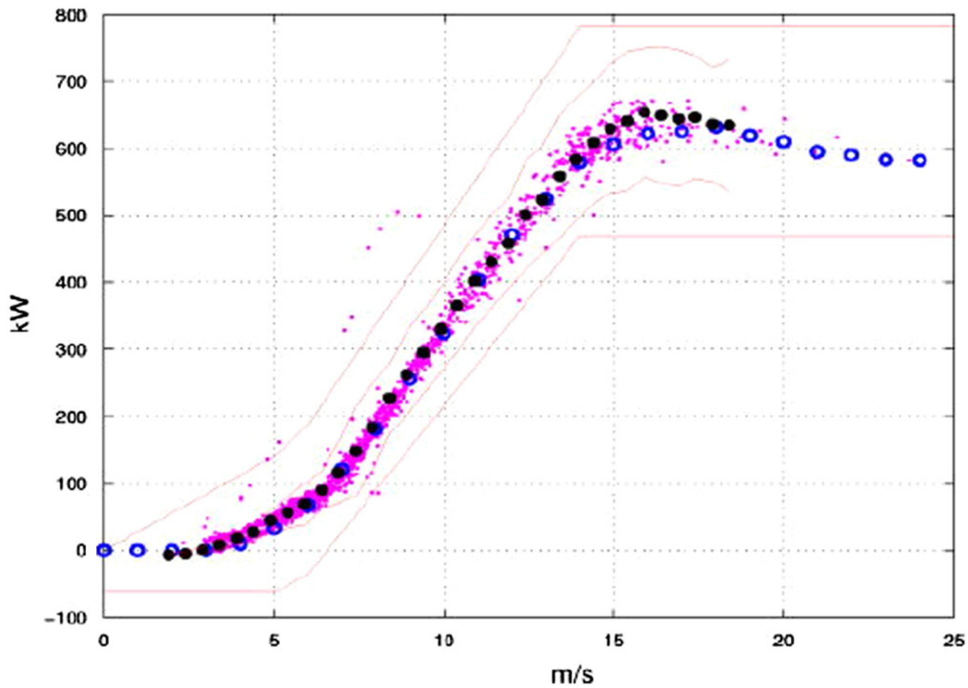


Fig. 4. Power characteristic of a 600 kW wind energy converter with absolute and calculated alarm limits.

To obtain this information from the raw data, 5-min mean values of wind speed and power are calculated out of every 3000 samples of the 10 Hz raw data (1):

$$\bar{\upsilon}_W = \frac{\sum_{i=1}^{3000} \upsilon_{Wi}}{3000} \quad \text{and} \quad \bar{P} = \frac{\sum_{i=1}^{3000} P_i}{3000}, \tag{1}$$

where $\bar{\upsilon}_W$ is 5-min mean value of wind speed and $\bar{P}$ is 5-min mean value of WEC active power, respectively.

These mean values are subsequently classified and to monitor the overall rotor performance, only deviations from the faultless condition have to be taken into account. Therefore, to perform the monitoring task, the faultless rotor condition has to be learned. This is realized by performing a learning phase. During this learning phase pairs of 5-min mean values $\bar{P}$, $\bar{\upsilon}_W$ are classified with a bin width of 0.5 m/s wind speed. Then the class mean value $\bar{P}_{Class}$ (classified 5-min mean value of active power) and the standard deviation $\sigma(\bar{P})$ in each class are calculated. The resulting curve $\bar{P}_{Class}$ ($\bar{\upsilon}_W$) is called power characteristic of the WEC.

As soon as the learning phase is completed, alarm limits will be calculated and the monitoring phase starts. Fig. 4 shows a power characteristic of a 600 kW WEC with stall power limitation. The small dots result from pairs of $\bar{P}$, $\bar{\upsilon}_W$ and the bold dots represent the calculated (''learned'') class mean values $\bar{P}_{Class}$. The circles represent the certified power curve provided by the WEC manufacturer. The outer thin lines are absolute alarm limits, which have to be determined by an application programmer of the used CMS. The inner thin lines are calculated alarm limits. The distance of the calculated (inner) alarm limits (named here as L_{dist}) to the class mean values.

$\bar{P}_{Class}$ have to be determined by an application programmer who sets up the CMS. For definition of the distances a heuristic approach can be chosen.

To avoid false alarms caused by one extreme measurement value of $\bar{P}$, a threshold criteria is used. A compromise between the robustness of the algorithm against extreme data points causing false alarms and the reaction time in case of a fault must be found. A number of 3 subsequent alarm limit overruns (corresponding to a reaction time of 15 min) will give reasonable threshold criteria in this respect. This means that if the fourth subsequent value of $\bar{P}$ exceeds an alarm limit, a problem with the rotor performance is detected and an alarming action is triggered by the CMS.

Spectral analysis and order analysis [20]: To analyze periodic nacelle oscillations, FFT algorithm has been used. For constant speed WECs, the FFT algorithm is directly applied to the measured acceleration time signals $a(t)$. To analyze nacelle oscillations of variable speed WEC, a modified algorithm has to be used which is called order analysis. This algorithm is based on samples recorded at equidistant rotational angles φ_R instead of equidistant time samples. If the measurement equipment does not allow proper samples directly triggered according to the rotor angle φ_R, the required data samples for order analysis can be generated by applying an interpolation algorithm to the time series of the acceleration signals. This algorithm uses the rotor position signal as a reference. The continuous variables t and φ are replaced by their time discrete counterparts defined by the sample time T and the sample angle Φ_R:

$$a(kT) \overset{\text{Interpolation}}{\longrightarrow} a(k\Phi_R). \tag{2}$$

Applying the FFT algorithm to $a(k\Phi_R)$ generates the complex discrete order spectrum $A(f_O)$ with the discrete "order frequency" f_O as the abscissa.

The frequencies of nacelle oscillations to be evaluated are quite small (about 0.1–3 Hz for large wind turbines). To evaluate these low frequencies with a reasonable spectral resolution Δf, the time window length T_{WIN} for the FFT and order analysis should be at least 100 s ($\Delta f = 1/T_{WIN}$).

To monitor the 1p (i.e., at the rotational frequency of the rotor) nacelle oscillations of a WEC, amplitude and phase of the 1p spectral components have to be analyzed.

Trend analysis and alarm generation for complex values require special algorithms. To monitor 1p nacelle oscillations, both amplitude and phase of the complex spectral components have to be analyzed. Fig. 5 shows the principle functionality of a trend analysis and alarm generation algorithm for monitoring complex spectral components. To monitor amplitude and phase simultaneously, the alarm limit is represented by a circle around the tip of the complex mean value X_0, which represents the faultless condition of the rotor. With the proposed circle shaped alarm limit changes in phase with constant amplitude represented by $dX_1 = X_1 - X_0$ will be detected as well as amplitude deviation without significant phase shift given by $dX_2 = X_2 - X_0$. Since these two extreme conditions for changes of complex values are covered, obviously all other changes in between the two extremes will be also recognized by the algorithm.

X_0 results from a learning phase, which is performed under faultless condition of the rotor to be monitored. In this phase the incoming complex values X_i will be averaged by averaging the real part and imaginary part separately.

The radius r_{AL} of the alarm limit circle is calculated as a multiple of the standard deviation of X_0:

$$r_{AL} = K \max(\sigma(\mathrm{Re}(X_0)), \sigma(\mathrm{Im}\{X_0\})), \tag{3}$$

where K is alarm limit tuning parameter.

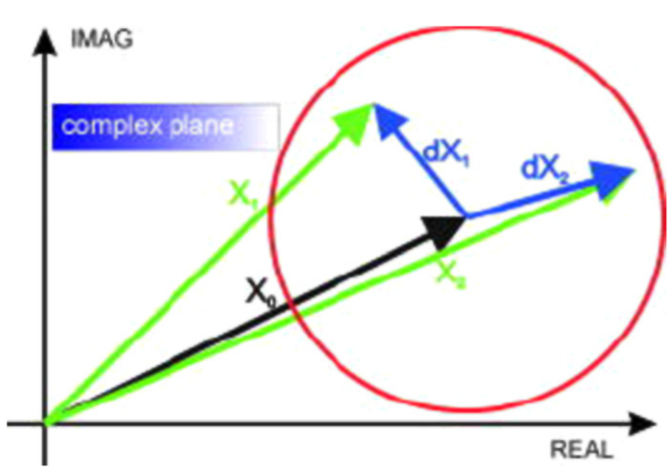


Fig. 5. Monitoring of complex spectral components with a circle shaped alarm limit.

To keep the calculation of radius r_{AL} simple, the maximum value of the two possible standard deviations is used. Experiences from field tests have recommended a value of 20 for the number N of averaged X_i in Eq. (3). For the parameter K in Eq. (3), a value between 3.5 and 4.5 is recommended.

An alarm is triggered, when the absolute value of the calculated difference $dX = X - X_0$ exceeds the alarm limit circle radius. As a threshold parameter, a number of 3 subsequent alarm limit overruns is required to cause the CMS to trigger an alarming action.

Fig. 6a shows WEC's power output during the experiments. Fig. (6b) shows the time history generated by applying a digital band-pass algorithm to the transverse acceleration sensor time signal of the 1p frequency transverse nacelle oscillation amplitude for the mass imbalance experiments. It can be seen that the amplitude is quite constant. Its magnitude is significantly higher in case of a rotor mass imbalance. The amplitude also depends clearly on the amount of mass attached to the rotor blade. In Fig. (6c), the amplitude of the 1p frequency of the torsional nacelle oscillation is shown. The experimental WEC is equipped with strain gauge sensors, so the tower torsion torque could be measured directly. The 1p amplitude time history again is generated using a digital band-pass algorithm. During aerodynamic asymmetry conditions, the amplitude is significantly higher.

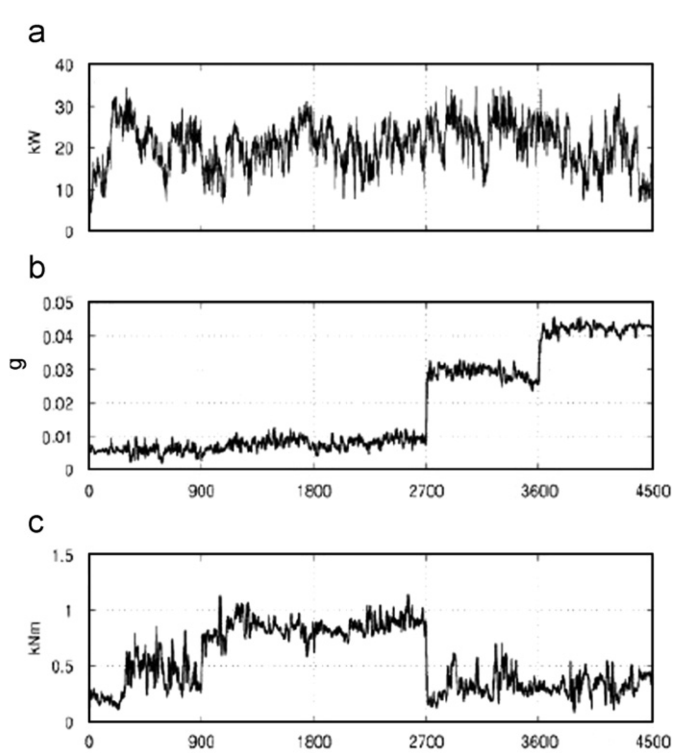


Fig. 6. (a) Five subsequent time series (900 s each) of electrical power output, (b) the respective 1p amplitudes of the transverse tower oscillation, and (c) the respective 1p amplitudes of the torsion tower bending moment.

Strain monitoring-based algorithm: Strain load on a certain body tries to deform or distort the shape due to material's internal structure. Internal resistance of the material to external load can be measured in terms of strain and some mechanism could be devised which will monitor the "strain rate" of that structure. By doing this, initiation of crack due to higher strain loads can be gauged and condition-based maintenance procedure can be started on the basis of severity of the impending fault.

Deformation sensors are used to locate the peak structural strain in the locales where the sensors are physically attached to the structure. Structural health monitoring can be carried out effectively by using peak strains in structures because these strains are occurred due to loads. By doing so, the location of damaged portion on the structure can be identified and appropriate strategies can be formulated for repair or replacing the component.

Considering the sensitive elements of SHM (CMS) system, strain sensors of one form or another are at the heart of many proposed schemes. They can be used for continuous load monitoring, allowing the structure's owner to build up an accurate picture of its usage. This information can be used to verify design assumptions about loading patterns or combined with fatigue models to predict residual life. An immediate application could be to indicate any exceptional load cases (buildings in earthquakes, airliners that have suffered hard landings), which may have caused damage, suggesting that the structure requires further detailed inspection [21].

Distributed temperature and strain sensor (DTSS) has been developed for structural monitoring by Sensornet. With DTSS, stresses and strains can be directly measured. It is capable of independently measuring strain and temperature at all points along a single length of optical fibre. FO technology has been used in it, which has flexibility and convenience for integrating sensing cables into practical structures. Wind turbine blade and mast stress measurement can be carried out with this technique [22].

Optical fibres-based algorithm: FO sensors are ideal for HMS (CMS) and superior over electrical strain gages because latter are not suited to use over many years because they are prone to failure by disbonding, creep or fatigue and the measurement of electronics drift with time. Although practical FO sensors are relatively new, it is beginning to be realized that they are going to be crucial for some SHM applications [21].

Mainly because of their lightning safety and neutrality to electro-magnetic interference, FO strain sensors are advantageously applied in wind turbine structural monitoring [23]. Out of the broad range of FO strain sensors, fibre Bragg grating (FBG) has the advantage of a direct physical correlation between the measured Bragg wavelength and strain. Recalibration of the sensors is not necessary, even after the signal-processing unit has been exchanged. The wavelength-encoded sensor signal cannot be disturbed by influences on the transmission lines, and their multiplexing in extended sensor networks provides results of spatial load distributions along very few optical fibre lines [24,25].

FBG measurement system is currently monitoring the 53 m long rotor blade of a 4.5 MW wind turbine in a wind park at Wilhelmshaven, Germany. The FGB sensor network is wavelength multiplexed; the Bragg wavelengths of the individual sensors in the network are measured utilizing broadband spectral illumination and spectrometric read-out of the sensor network reflection signals. The SPU has been developed as a robust and potentially low-cost instrument for operation in a heavy-loaded industrial or aerospace environment [26].

Bragg wavelengths are calculated as the result of a subpixel approximation (e.g., Gaussian correlation fit) to the intensities of ± 7 charge-coupled device (CCD) pixels around every sensor peak maximum in the reflected spectrum, corresponding to a spectral width of ± 0.6 nm. The sensitivity of the relative Bragg wavelength shift $\Delta\lambda_B/\lambda_B$ to the strain of the optical fibre (i.e., to its relative elongation $\Delta L/L$) depends on the fibre's effective photoelastic coefficient p as the only experimental calibration parameter:

$$\frac{\Delta L}{L} = \frac{\Delta\lambda_B}{\lambda_B}(1-p). \tag{4}$$

The experimental value of p for the used fibre type, $p = 0.23$, has been measured once on a calibrated bending beam and was found to be constant within the operational strain, temperature and wavelength ranges, $\pm 5000\,\mu\varepsilon$, -40 to $+180\,°C$ and 800–860 nm, respectively [27].

FBGs as intrinsic FO strain sensors can be embedded directly into the glass fibre-reinforced plastics (GFRP) of the rotor blade, without major disturbances of the laminate. However, in this test installation, the FBG strain sensors have been integrated after finishing the rotor blade as shown in Fig. 7 [27].

Three strain sensor, pads each has been attached to both the windward and the leeward internal surfaces of the blade on opposite symmetrical positions are shown in Fig. 8 [27].

The strain load of sensor D1.1 at a position near the rotor shaft (Fig. 8, curve 1, and leeward position 1) has nearly sinusoidal characteristics, varying synchronously with the blade position during rotation. Contrary to curve 1, the strain response near the blade tip (sensor responses in

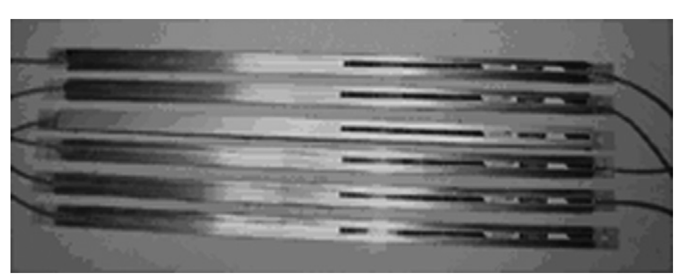


Fig. 7. Photograph of six sensors pads for strain monitoring in the rotor blade. The third pad includes a temperature sensor.

curves 2 and 3 in Fig. 9) shows more structured characteristics, additionally consisting of higher as well as lower frequency components. The anti-symmetric responses from the opposed sensors D1.3 and D3.3 indicate this strain also has a localized flap-wise bending behavior, with superimposed wobbling near the free blade tips.

Fig. 10 shows the load relations between strain sensors at different positions during an acceleration period of the wind turbine, with exact calibration of their zero strain values.

Inertial sensing [28]: Inertial sensors detect linear acceleration or angular motion. Damages will inevitably affect the modal dynamics of a wind turbine blade. It is noted that linear acceleration may be measured up to 9 g and angular acceleration up to 5300 °C/s^2. The single components sensor and angular rate sensors are being developed for low cost applications and are available in market.

A conceptual layout for a system could be as indicated in Fig. 11. The placement is based on likely positions for

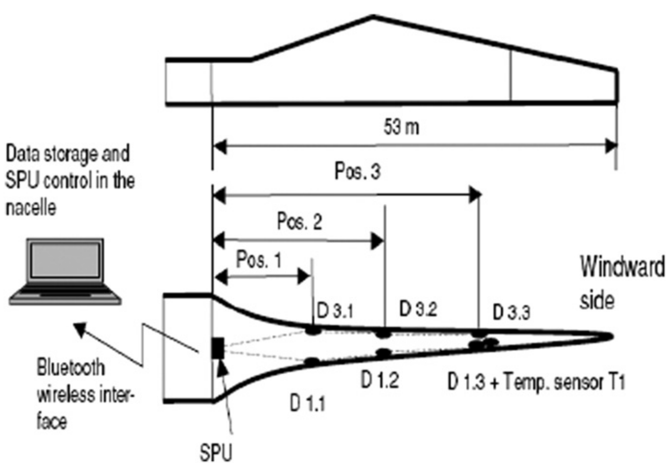


Fig. 8. Scheme of positions of sensor pads and signal-processing unit (SPU) in the rotor blade.

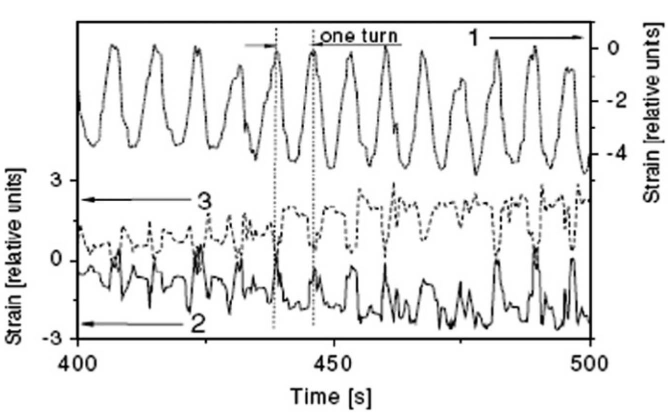


Fig. 9. E112 operating at 8.4 rpm. Example of strain measurement results using 50 Hz FBG interrogation unit StrainaTemp50. (1) Sensor D1.1 on leeward blade side, near to rotor shaft at position 1. (2, 3) Sensor pair D1.3 and D3.3 on opposite leeward and windward blade sides, respectively, near to the tip of blade at position 3 (definition of sensor positions in Fig. 8).

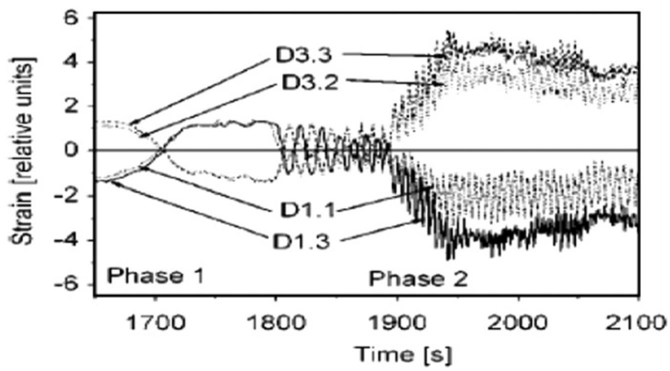


Fig. 10. Results of load monitoring during acceleration of the turbine. Phase 1: slow rotation at 0.3 rpm; blades are loaded only by their own mass. Phase 2: acceleration to 11 rpm; blade bending under changing wind load (definition of sensor positions in Fig. 8).

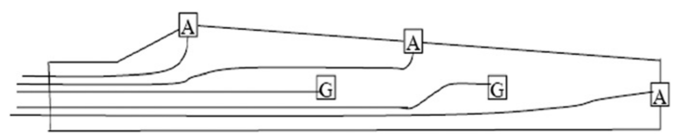


Fig. 11. A wind turbine blade with estimated positions of acceleration sensors (A) and rotational rate sensors (G) for monitoring the modal dynamic of the blade.

acceleration—linear and rotational—for estimation of modal dynamics. Low number of sensors (here five) can be relied on the hypothesis of low-order modes to be detected and on the basis of this procedure, all extended region of the blade will provide weighted—contributions to the signals. Thus, all extended regions are in principle be monitored intrinsically.

The signals from the inertial sensors will be relatively narrowband. If damage occurs both frequency and amplitude will change. A tracking band-pass filter (e.g., implemented with a common phase-locked loop) can be used in the estimation of these processes. The demodulated signals could then be correlated with the signal from an anemometer in order to compensate for variations in wind load. The correlations would then be used as parameters in a fitting procedure using a general model for the modal dynamics of the blade. A decision-making processor would then determine if damage had occurred.

The most uncertain part of this method for damage detection is believed to be associated with the algorithms and procedures for data processing.

Optical coherence tomography (*OCT*) [28]: It is relatively new diagnostic tool and its basic method has similarities with ultrasonic detection. A focused beam is scanned over the target. The depth resolution is not obtained by a direct measurement of the time-of-flight—but by using light with a very short coherence length (1–50 μm). (A direct measurement of the time-of-flight would require femtosecond resolution.) The reflected light is interferometrically compared with reference light from the same light

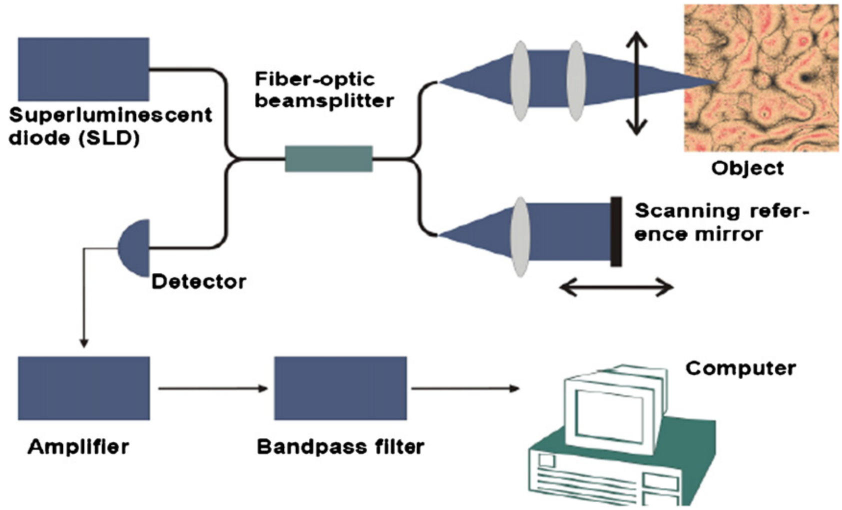


Fig. 12. Optical coherence tomography system.

source. By scanning the optical delay in the reference beam, an image of the depth structure can be obtained. Structural elements down to 1 μm can be resolved, although typical light sources will give a resolution about 10–50 μm. The scheme is presented in Fig. 12.

OCT can also be implemented in a configuration where velocity or displacements are measured. This implies that OCT can also be used for detecting acoustic emissions (AEs) as well as more steady flow phenomena.

The method has been applied by National Institute of Standards and Technology (NIST) to investigate both of the fabrication of composite materials and for the detection of damages in composites [72]. The blade of WEC is made of composites and this technology can be applied to monitor the fabrication and operation of rotor blade.

Bicoherence based on electrical power: For this type of condition monitoring to be successful, small physical changes in the machine must be detected from a very noisy signal. If some feature of the signal amplifies the change and provides a reliable signature, then detection is made easier. Presence or absence of phase coupling between frequency components of the signal may provide such a signature. Since the power spectral density (PSD) discards phase information, it cannot detect the presence of phase coupling. The bispectrum, a third-order spectral statistic, detects phase coupling, but its magnitude varies with the power in the signal and therefore is not convenient for detection purposes. Bicoherence, a normalized bispectrum, overcomes this problem [29].

Since the magnitude of the bispectrum varies according to the power spectrum of a signal, it can be useful to normalize the bispectrum by the power spectrum. This is variously called the 'bicoherency' [30], the 'skewness function' [31], or simply the 'bicoherence' [32], and is defined as

$$b_x(\omega_1, \omega_2) = \frac{B_x(\omega_1, \omega_2)}{\sqrt{S_x(\omega_1)S_x(\omega_2)S_x(\omega_1 + \omega_2)}}. \quad (5)$$

Sometimes a slightly different denominator is used where

$$S_x(\omega_1)S_x(\omega_2) = E[X(\omega_1)X^*(\omega_1)]E[X(\omega_2)X^*(\omega_2)] \quad (6)$$

is replaced with [33]. Often the magnitude or magnitude squared of Eq. (5) is referred to as the bicoherence [34]. Combining the estimates of the PSD and the bispectrum yields the estimate for the bicoherence b [30].

$$\hat{b}_x(k, l) = \frac{E[X_k X_l X^*_{k+1}]}{\sqrt{E[X_k X^*_k]E[X_l X^*_l]E[X_{k+1} X^*_{k+1}]}}. \quad (7)$$

The magnitude of the bicoherence indicates how much of the power in a frequency component is due to phase coupling with two other components. Noise in the signal dilutes the phase coupling and reduces the value of the bicoherence.

Coherence between blade tip motion and electrical power output gives the degree of linear relationship between the two as a function of frequency. The results of the estimate, shown in Fig. 13, show high coherence at the rate of rotation, 0.64 Hz, and two other broad peaks centered at 2 and 3.7 Hz.

Thus, a direct coupling of tip motion to power output is confirmed, at least at selected frequencies.

AE based on pattern recognition [35]: A methodology for wind turbine blade monitoring using AE detection of damage processes in the structure has been developed by AEGIS (given the name from the word aegis, means protection) consortium, supported by the European Commission. The methodology has been developed separately for the peak load events and the more usual operational fatigue loading and can be applied as an enhancement to the conventional blade certification test and has the potential to be adapted to large-scale field application of the techniques on operational wind turbines.

In AE monitoring, surface-mounted piezoelectric sensors detect and locate the origin of sound waves within a structure. The system is very sensitive and can detect much weaker signals, mainly in the non-audible frequency

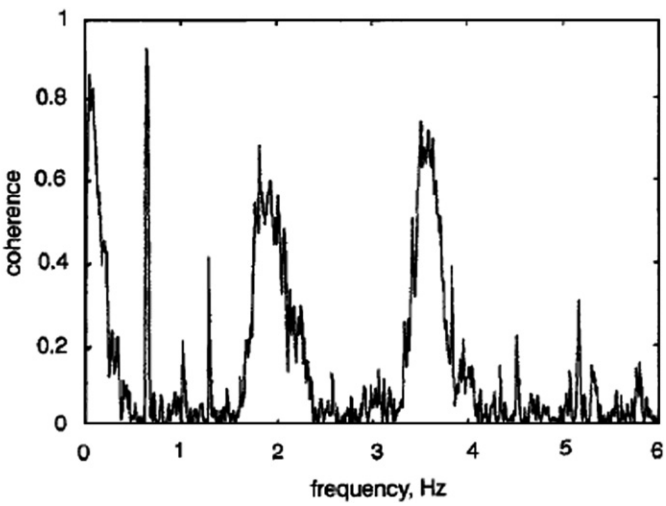


Fig. 13. Coherence of flapwise tip acceleration to electrical power output (matched blades).

domain (20–1200 kHz). The signals can be characterized in terms of features such as Amplitude and Energy and inferences made about the kinds of damage process taking place in the blade. AE monitoring can determine the location and sometimes the kind of damage, which is taking place; it can also be used to determine damage criticality for a given load, but conventionally this has required the application of long-sustained loads at this particular level.

Aegis PR is a Pattern Recognition Software suite developed within the AEGIS project to analyze and classify AE data from wind turbine blade tests. It is capable of performing unsupervised (UPR) and supervised (SPR) pattern recognition as well as classical AE data analysis. The Aegis PR software algorithms mathematically segregate the AE data based on their AE features and, ultimately, provide a grade for the structural integrity of discrete wind turbine blade sections according to user-selectable criteria based on the level of AE activity and/or the presence of trends in particular ''families'' of AE data. The Aegis PR software uses mathematical clustering algorithms in order to divide each set of AE hits into families called ''clusters'', based on the similarity of their features.

The acoustic emission loading (AEL) test, coupled with the AEGIS PR software, has been demonstrated to give a very good indication of damage criticality. AEGIS is applied to test the fatigue loads on the blades and the results are demonstrated in Fig. 14.The static test methodology is applied with rope and pulley method to test the blades in-service and results are presented in Fig. 15.

AE monitoring could, in principle, be applied across a whole wind farm.

AE based on continuous sensor [36]: The continuous sensor performance was analyzed and validated using simulated AE signals, namely those caused by pencil lead breaks. The advantage of the continuous sensor configuration for monitoring actual AE signals generated by fatigue damage growth in a composite specimen is determined. The central section of the specimen had two semicircular notches of 0.25-in (6.325 mm) radii. The specimen is initially subjected to fatigue until a visible crack appeared at one of the edges. The arrangement of sensors on the specimen is shown in Fig. 16. This specimen is instrumented with a surface-bonded continuous sensor as shown in Fig. 17. The first node of the continuous sensor is at a distance of 0.625 in (15.81 mm) from the fatigue damage site. In addition, two conventional sensors are also attached to the specimen. The sensors S1 and S2 are 0.25-in (6.325 mm) damped ultrasonic sensors with a resonant frequency of 5 MHz. These sensors are chosen for their suitability in terms of wide band non-resonant response needed for quantifying AE signals, based on an earlier study.

The specimen is subjected to a fatigue loading with a mean load of 750 lb (3336.16 N) and amplitude of 500 lb (2224.11 N).

Fig. 18 shows the waveforms of the AE signals obtained during the fatigue loading. The amplitudes of the signals from the continuous sensor are much larger than the signals from the conventional sensor. These differences can be attributed to the frequency responses of the two types of sensors, their relative sizes, and to the fact that surface bonded or embedded sensors are likely to be more sensitive to the AE signals compared to the conventional sensors. The AE signal sensed by the conventional sensors S2 is much smaller in amplitude compared to that from an identical sensor S1, which is merely 3 in (75.9 mm) closer to the damage site. Furthermore, the high-frequency components present in the signal from S1 are absent in the signals from the sensor S2. This variation in the signal characteristics over as short a distance as 3 in (75.9 mm) in composite media illustrates the need for multiple sensor nodes in critical regions for the accurate detection of damage magnitudes and rates.

Structural neural systems (SNS) [36]: The SNS detects damage early and multiple damage sites on the blade are identified well before the catastrophic failure of the blade. Strain gages on the blade indicated damage at various locations just before buckling failure. The damage location predictions using the SNS are shown in Fig. 19 and are approximately verified based on the locations of strain gages. Continuous sensors are also placed on the top and bottom of the blade and signals are recorded independent of the SNS. The continuous sensors are connected to a commercial AE monitoring system. The continuous sensors detected more AEs than the SNS due to the lower settings for signal acquisition. The continuous sensors successfully detected damage early and tracked the AE occurrences during the damage growth. Details of the testing are given in Ref. [37].

The results of the test demonstrated that the SNS is a viable method for SHM of complex composite structures.

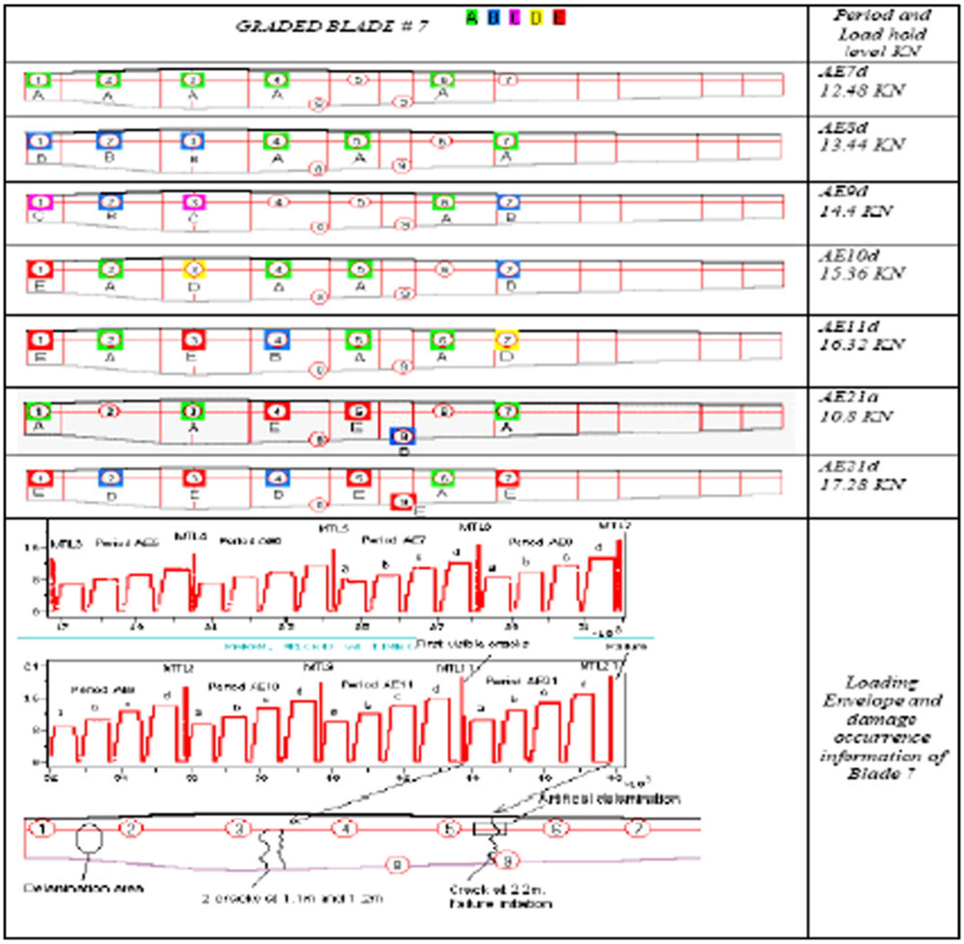


Fig. 14. Aegis PR software grading for small blade 7s.

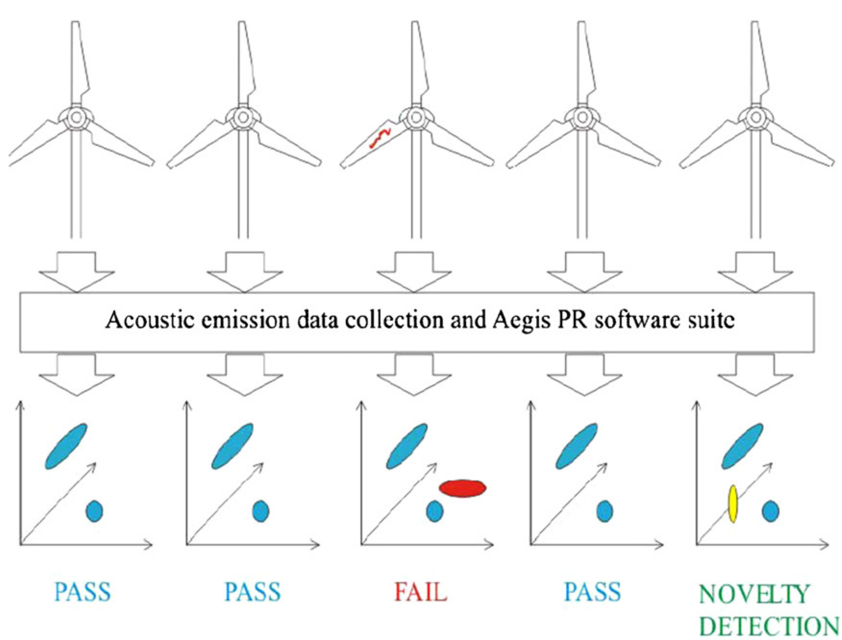


Fig. 15. Application of Aegis PR software to identify AE patterns with known damage implications or novel parameter patterns for future investigation and learning.

A larger SNS can be applied on a wind turbine blade during fatigue testing, and to test the SNS on other components of the wind turbine.

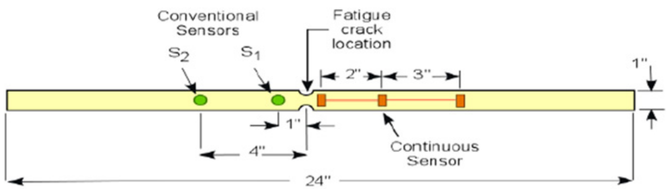


Fig. 16. Composite specimen with fatigue damage.

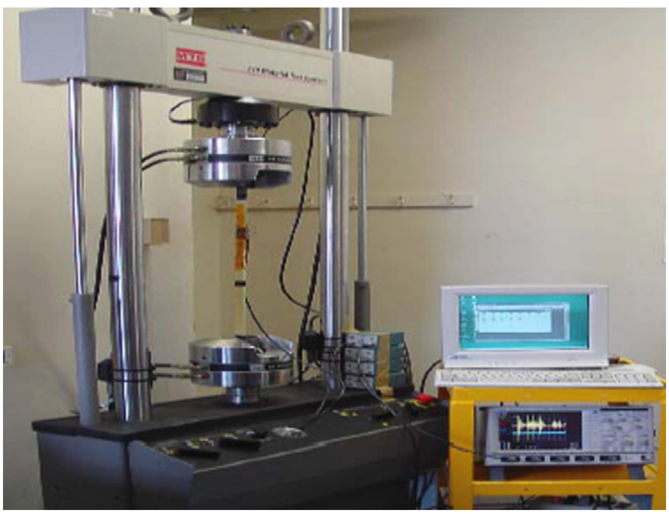


Fig. 17. Test setup for monitoring the damage growth with a continuous sensor.

Vibration/stress wave [36]: The vibration/stress wave monitoring is used for the detection of buckling under more controlled conditions. A composite bar is instrumented with two lead zirconate titanate (PZT) patches as shown in Fig. 20. The specimen is first supported in the straight unbuckled condition and then both ends are clamped. The left end of the bar is to be kept stationary while the right end of the plate is translated to introduce the desired level of buckling. The central buckling displacement is measured using a ruler. The clamping force is accurately controlled by using torque wrenches.

The instrumentation used for introducing vibration into the specimen and for monitoring the amplitude of the vibrations is shown in Fig. 21. It consists of an arbitrary function generator and a power amplifier, which delivers gated sine pulses to the transmitting PZT patch on the bar. The signal from the receiving PZT patch is collected directly in a digital oscilloscope and transferred to the personal computer (PC). One of the frequencies that provided good indications of the buckling deformation is 72 Hz.

The signals from the receiving PZT patch are recorded when the buckling induces deflection at the mid point of the bar and finally, the bar is returned to its original unbuckled state and the vibration amplitude is again measured. Fig. 22 shows the comparison of the waveforms corresponding to the unbuckled state and various buckled states. The magnitude of the oscillations undergoes a drastic reduction as the buckling displacement increases. When the bar is returned to the unbuckled state, the signal amplitude returned to the initial unbuckled bar amplitude

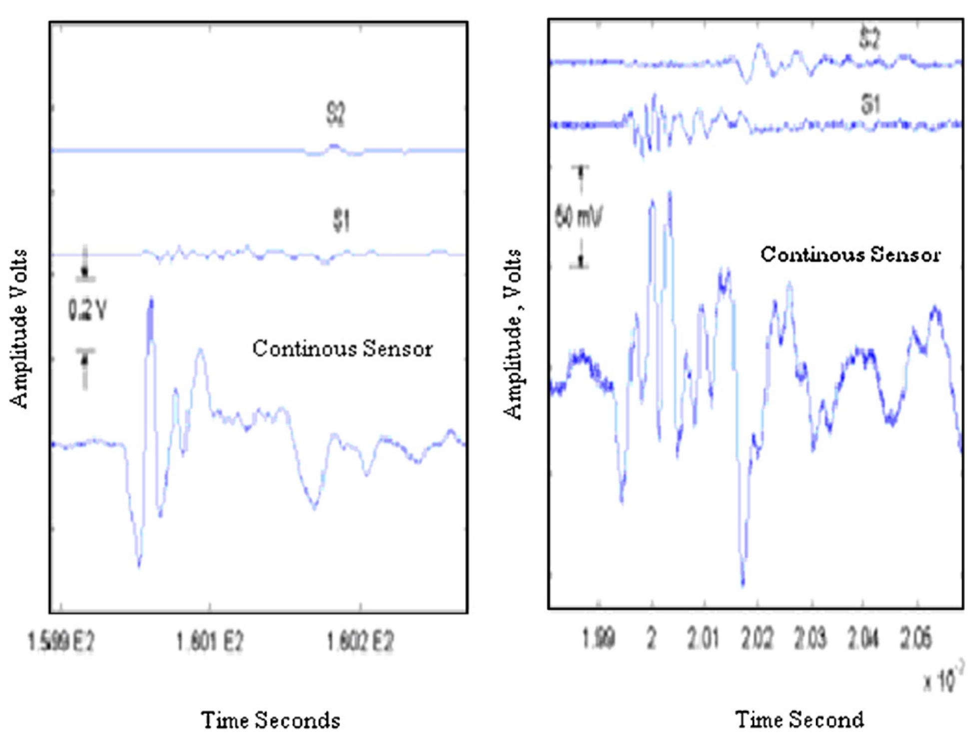


Fig. 18. Comparison of AE waveforms obtained by a continuous sensor and conventional sensors.

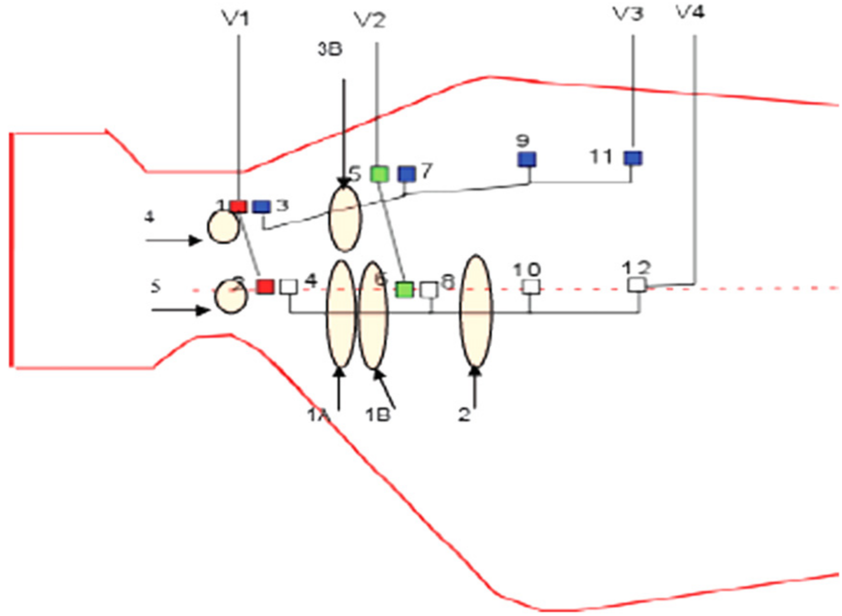


Fig. 19. Schematic of the SNS on the test wind turbine blade. The SNS has 4 neurons identified as V1, V2, V3, and V4. Damage was predicted in locations 1–5.

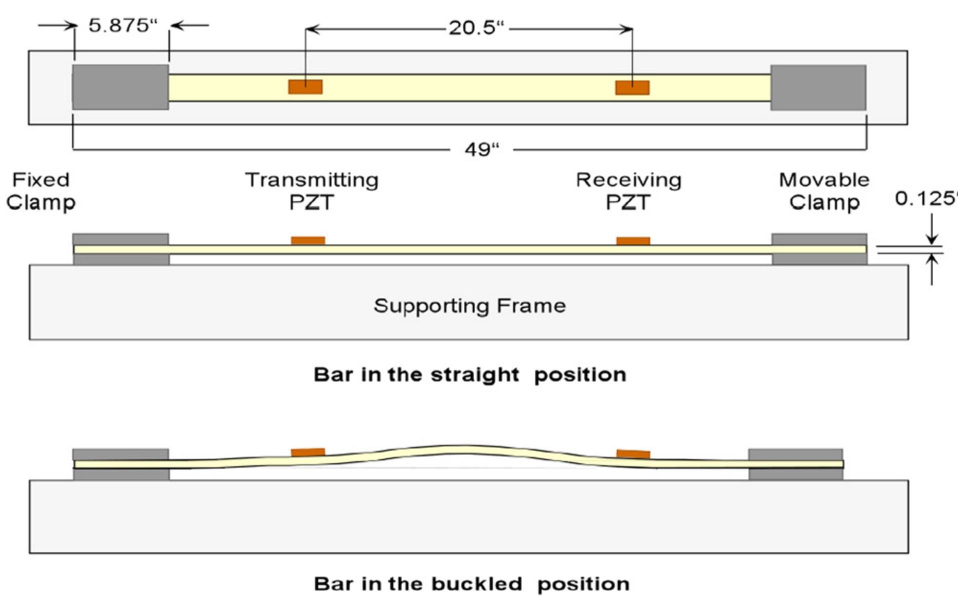


Fig. 20. Specimen used for buckling experiments.

as seen from Fig. 22, indicating that the changes in amplitude are indeed caused by the buckling deformation in the bar. In a second experiment, the bar is excited by sinusoidal chirp signals with various starting and ending frequencies. The results corresponding to a 3-s chirp with a starting frequency of 60 Hz and ending frequency of 120 Hz is shown in Fig. 23.

The frequency of oscillation at time $t = 0$, 1, 2 and 3 s are respectively 60, 80, 100 and 120 Hz. In general it could be seen that as the buckling deformation increases, the frequency of maximum amplitude for the bar, which originally was at about 76 Hz, gradually increases until it reached 112 Hz.

2.3.2.2. Pitch mechanism. Servomotors are used to control the pitch systems. Large turbines often have independent pitch control system. Overall safety of this system is realized by current measurement/time measurement and difference in pitch angle differences.

Model-based approach is adopted for CMS of this system because this approach is suitable for non-stationary components. Trend analysis is an emerging area to carry out CMS of pitch system.

Two approaches are applied to monitoring the pitch system:

Trend analysis (*process residual based*): The diagnosis can be based on the residual of the process and estimator

output signals (see Fig. 24). In this situation, a constant model is used. The difference between the output of the system and the output of the model can be monitored. Trend analysis of this residue can be used to detect changing characteristics of the system [17].

Trend analysis (*model parameters based*): Another possibility of model-based fault detection is continuous estimation of the model parameters, based on the measured I/O values and to monitor the trends in the parameters (see Fig. 25). The performance strongly depends on the accuracy of the estimation procedure. The number of I/O signals and the measurement accuracy of these signals are of importance to be able to detect changes in trends in an early stage [17].

2.3.2.3. Drive train. Condition monitoring of gearboxes and bearings is the state of the art in several industrial applications with rotating machines like, turbine machines. The monitoring systems used in these applications are, in general, based on vibration measurements. Often simple statistics of these measurements (e.g., maximum value) are calculated and trend analysis is applied to determine the machine condition. Advance methods are based on spectral analysis techniques to monitor frequencies that correspond to periodic excitations caused by specific faults, e.g., pitting on the outer face of a bearing [38].

2.3.2.4. Gearbox. *Spectral analysis*: This method is especially well suited for gearbox diagnosis. The algorithm calculates the overall spectral energy (RMS value) in the side bands divided by the tooth mesh amplitude. In case of degrading quality of gearwheel teeth, the energy of the side bands and thus the ratio's values will rise. Fig. 26 shows in

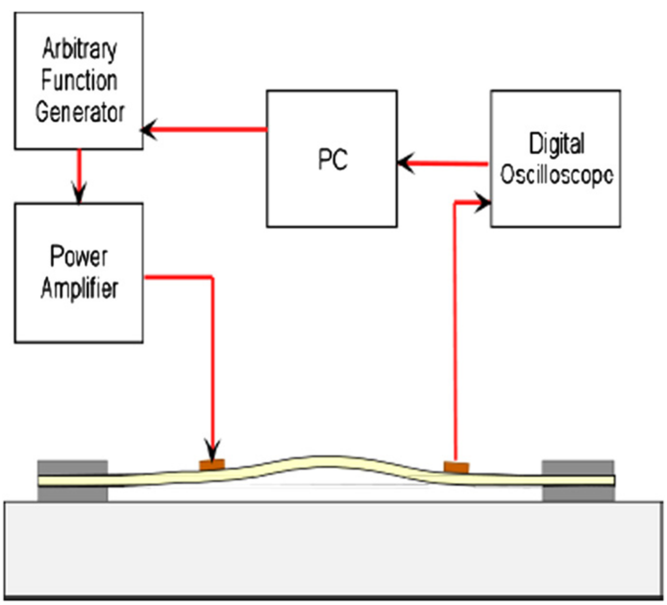


Fig. 21. Instrumentation used for measuring the specimen response.

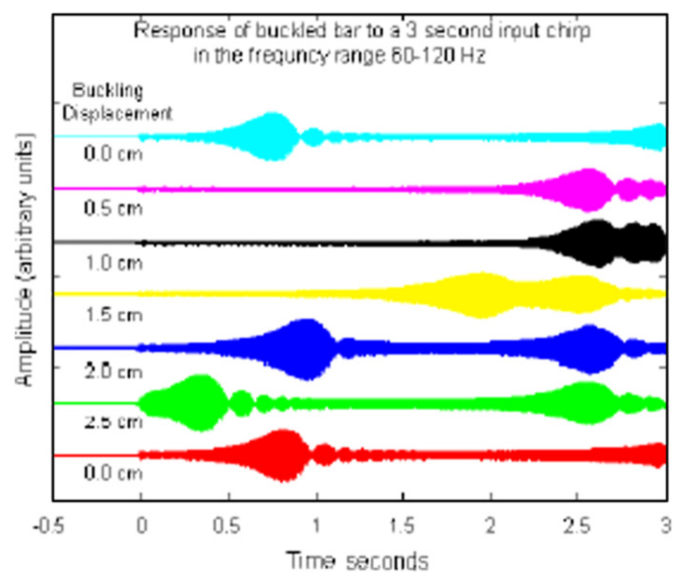


Fig. 23. Response of the buckled bar to chirp excitation.

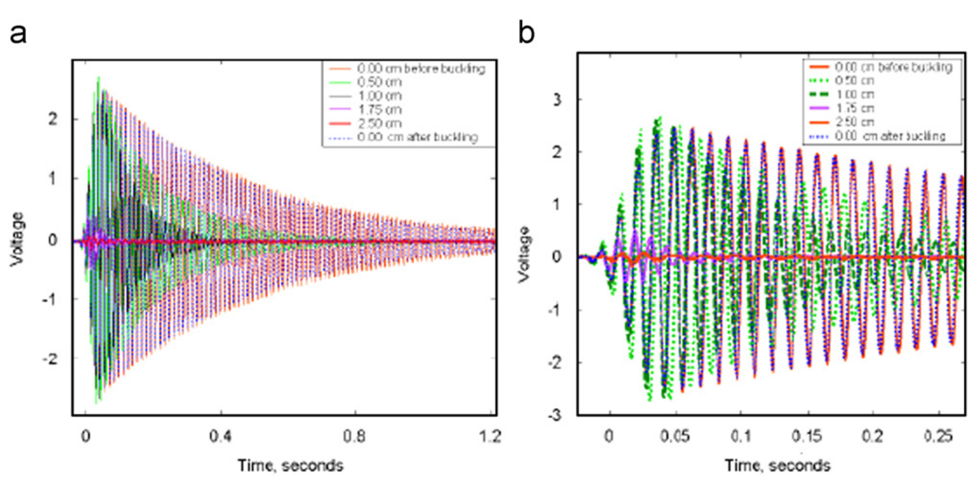


Fig. 22. Comparison of waveforms obtained in the unbuckled and buckled condition: (a) the complete waveforms and (b) the initial portion of the waveforms expanded.

diagram (a) the power density spectrum (PDS) of vibration at a 250 kW wind turbine gearbox. The dominating peak at 106.5 Hz is the tooth mesh frequency of the first planetary stage. The distance of the blade is 0.67 Hz, which is the rotational speed of the gearwheel's shaft. This way, faults can be detected by monitoring only one fault frequency. This type of signal analysis requires very detailed knowledge about the construction parameters of the WEC's gearbox and bearings. However, obtaining data is not an easy job during the project activities [39].

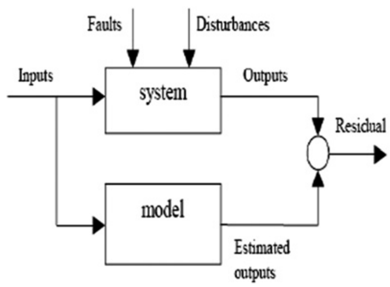


Fig. 24. Fault estimation based in residual.

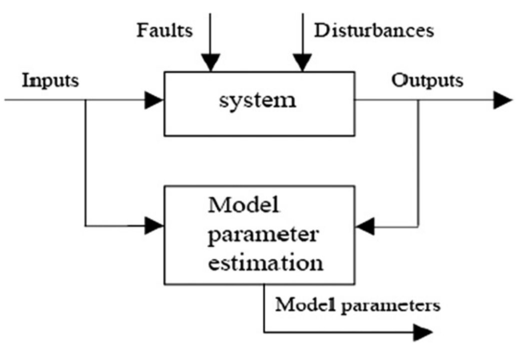


Fig. 25. Fault estimation based on model parameters.

Some of the spectral components of the gearbox vibration can be found in the PDS of the generator vibration too (Fig. 26b). The knowledge of such components is used to eliminate these influences out of generator vibration analysis [39].

Cepstrum analysis [40]: It is the advance method for monitoring the faults and is especially suited for gearbox diagnosis. Fig. 27 shows the PDS and the cepstrum of the gearbox vibration of a 250 kW wind turbine. Strong harmonics due to defect in a planetary stage are reflected in one peak of the cepstrum. This way, the fault can be detected by monitoring only one fault frequency.

2.3.2.5. Gearbox and bearings. *Spectral analysis*: Modern-type WECs are based on rotational components. Therefore, measurement of vibration on component housing and structural oscillation will yield data for the calculation of the characteristics of the wind power turbine [41]. The sensors measure the acceleration at different places in the turbine. By measuring the acceleration and then integrating it once or twice, one obtains the velocity and the displacement. Components that vibrate are a sign of malfunction and by simply looking at the displacement of the component the vibration can be measured [9].

Another way of analyzing the data from the sensors is by looking at frequency spectrums. Vibration and oscillation data time series are analyzed and evaluated using spectral analysis algorithms. These algorithms are based on the fast

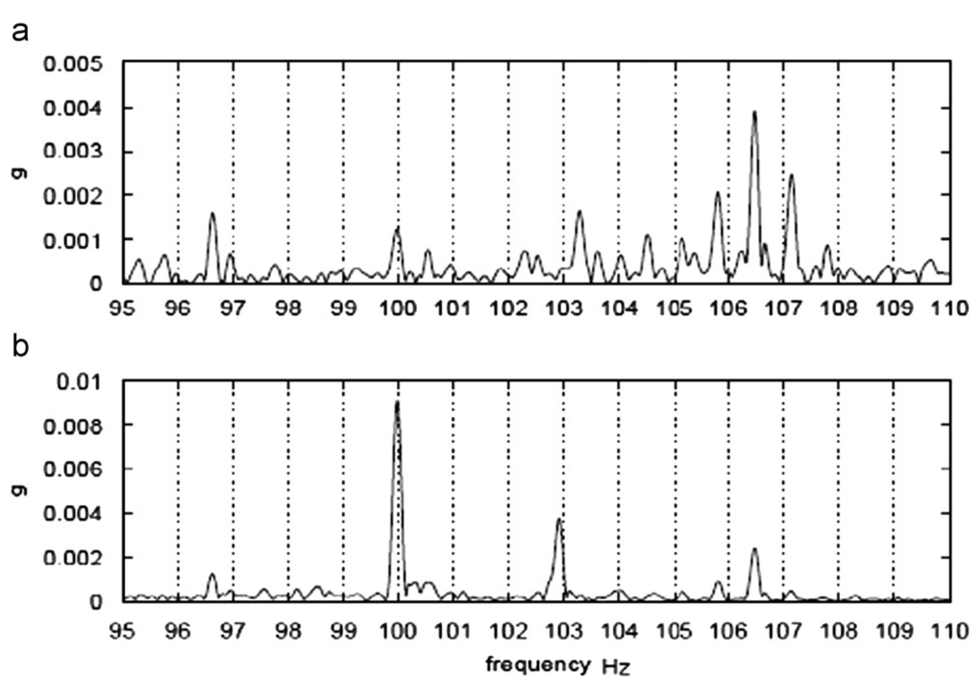


Fig. 26. Spectral analysis of vibration signals (a) power density spectrum of gearbox vibration and (b) PDS of vibration at the generator bearing.

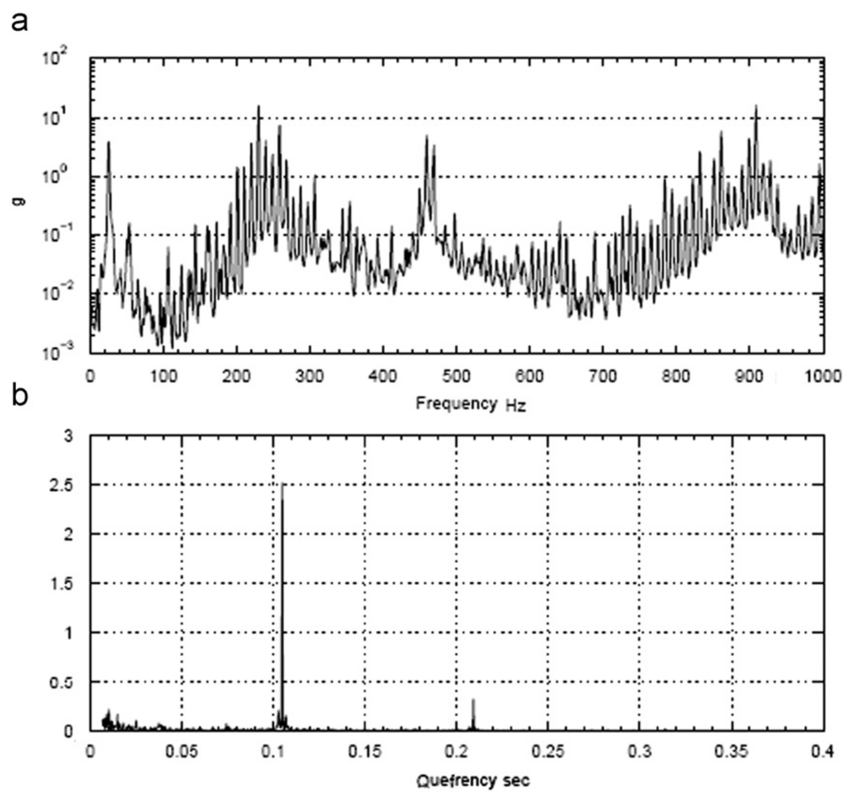


Fig. 27. Spectral analysis of gearbox vibration: (a) power density spectrum and (b) cepstrum of spectral harmonics.

Fourier transform (FFT) functions, which are common in digital data evaluation [41]. These spectrums will tell you which vibrations are caused by the ordinary rotating parts in the WEC and also which vibrations are caused by potential wear or damage on the turbine, the bearings or the gears.

When damage occurs to a bearing, small vibrations occur in the housing of the bearing. The frequency of the vibrations is depending on the revolution of the shaft but also on the type of bearing. If one has exact knowledge of what type of bearing is used and the speed of revolution one can analyze the frequency spectrum and thereby tell what part of the bearing that has been damaged [13].

The spectrum analysis can also identify alignment problems, which are claimed to be a major factor of shortening the lifetime of the turbine. The modern CMS equipment and software are now able to analyze the data and give a hint to what might cause the problem [9].

Envelope curve analysis: It is an efficient technique for gearbox and bearings fault detection [20]. This method analyses the modulation of high-frequency oscillations (above 10 kHz) by low-frequency excitations resulting from certain faults. Fig. 28 shows a power spectrum and an envelope curve spectrum for the generator vibration signal. It can be seen that the spectral component at 103 Hz, which is dominant in the envelope curve spectrum, is only a small peak in the power spectrum near the high amplitude of twice the grid frequency [38].

From the generator bearing data, it can be concluded that this frequency component is caused by the impulses emitted from the balls passing a faulty position (emitting) on the outer face of the bearing. The energy of these impulses is quite low but their spectrum contains very high-frequency components. Therefore, the analysis of modulation in high-frequency ranges is especially well suited to detect this type of impulse signals [38].

2.3.2.6. Electrical system. *Generator* [43]: The reduction of operational and maintenance costs is continuously required of modern wind generators. In particular, with plans for extending wind farms at sea (making the generators more inaccessible), it is required to increase reliability and production time, simultaneously with an increase of service interval. An important factor enabling this is to provide wind generators with advanced CMSs and monitoring the generator during operation to avoid undesirable operating conditions, and to detect incipient faults in the components.

Many sources show that bearing faults and stator insulation breakdown causes the majority of machine failures. For small induction machines, the stator winding insulation degradation is one of the major causes. Failure surveys have reported that percentage failure by components in induction machines is typically: bearing related (40%), stator related (38%), rotor related (10%), and others (12%) [44].

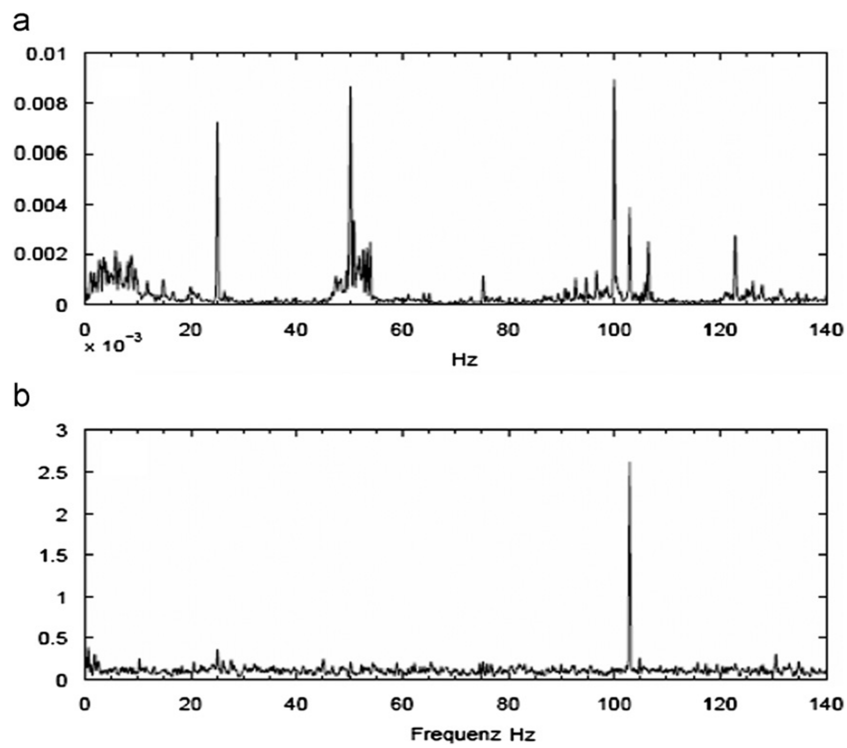


Fig. 28. (a) Spectrum and (b) envelope curve spectrum of the vibration signal of a generator bearing with a minor fault.

The most important component of the measurement system is a complete CMS, which comprises many subsystems like transducers, signal conditioning boxes and data acquisition devices, as can be seen in Fig. 29.

The induction generator has been monitored using measurements of stator and rotor currents, stator voltages, rotor speed and temperature in the windings.

Time-domain analysis [43]: Time-domain analysis using characteristic values to determine changes by trend setting and for extracting the amplitude information from current signals is a good means to monitor the condition of stator and rotor of the generator.

The faults like stator phase inductive unbalance and phase resistive unbalance; rotor phase resistive unbalance and turn-to-turn fault are being identified by using current signals are shown in Fig. 30.

The measurements are acquired by a Tektronix Oscilloscope-TDS 540 and by the DAQ device—ICS 645 via Matlab software. The doubly fed induction generator (DFIG) is operating, during the measurements, at a rotor speed of 1475 rpm corresponding to a stator active power of 2 kW.

The pictures below (Figs. 31 and 32) show the rotor and stator currents of the generator measured under a resistive unbalance ($R_v = 1.2\,\Omega$) in one rotor phase of the same value as the rotor phase resistance, corresponding to a stator power of 2 kW. A very small difference exists in both stator and rotor currents and can only be due to the unbalance provoked.

Similarly, the degree of unbalance provoked in one stator phase, through introducing the inductive unbalance

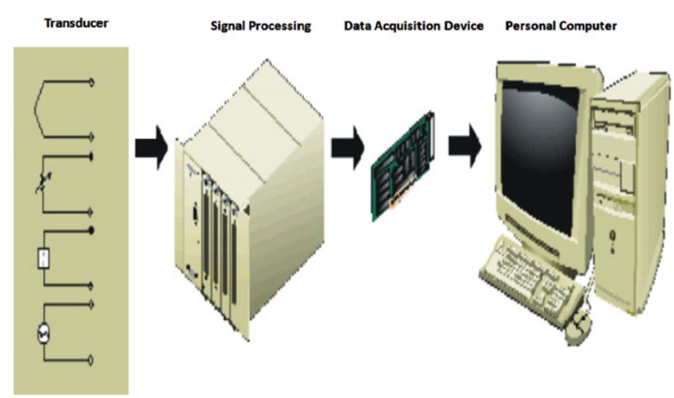


Fig. 29. The block diagram of CMS.

can be reflected in stator currents. Moreover, the stator and rotor currents of the generator that corresponds to stator power of 2 kW, under turn-to-turn fault developed in one stator phase, illustrate that the rotor currents (RMS values) have almost the same value as of current. Hence, the stator current could be a good indicator in detection of turn-to-turn faults.

3. FDS, methodology and algorithms

3.1. FDS

The implementation of FDS is critical for an early detection of faults and getting necessary time to prepare

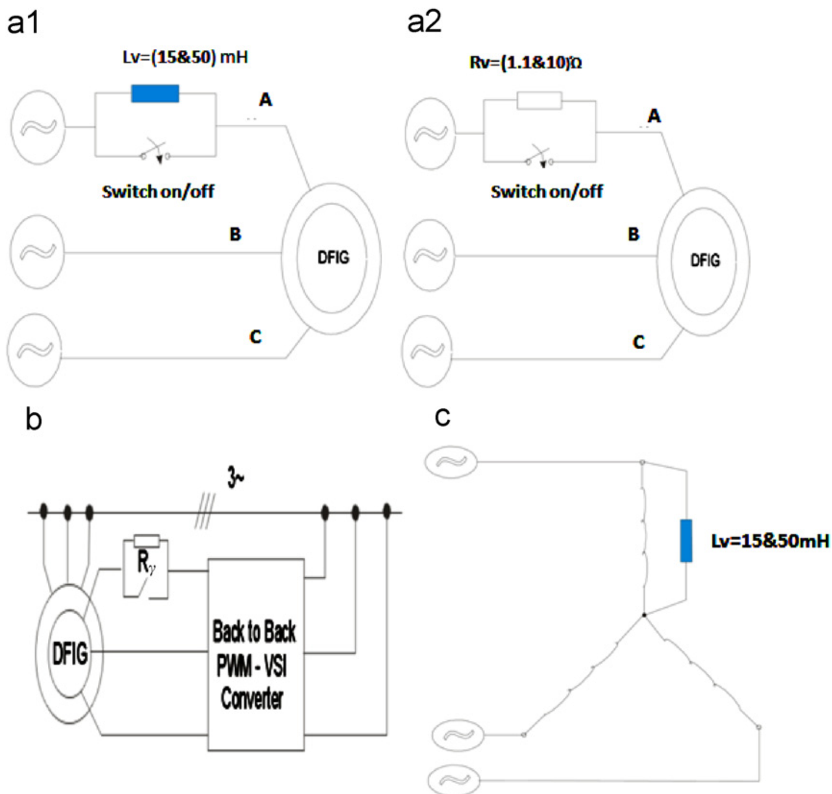


Fig. 30. (a1) One stator phase inductive unbalance; (a2) One stator phase resistive unbalance; (b) One rotor phase resistive unbalance and (c) Turn-to-turn fault.

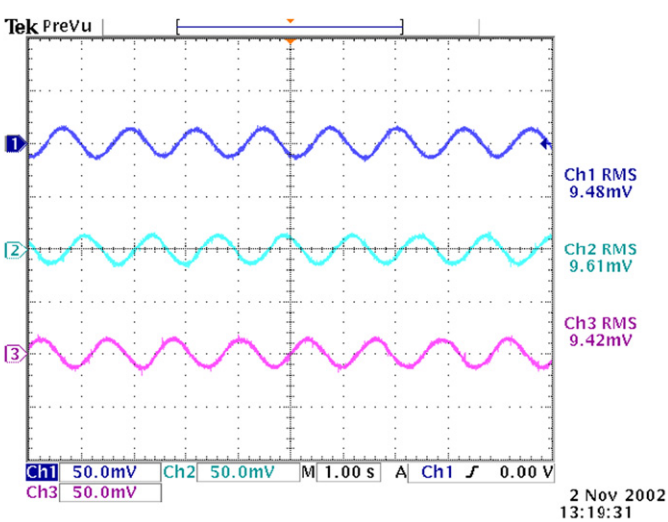


Fig. 31. The rotor currents of DFIG acquired by TDS 540 under the resistive unbalance of 1.2 Ω in one rotor phase at 2 kW. Scaling factor is 4 mV/A.

maintenance schedule to arrange spare parts and related logistics especially for offshore turbines, which are normally located farther and, in remote locations.

A signal-processing unit (SPU) evaluates process measurements to extract characteristic parameters, which indicate fault situations. The parameters are further processed by a classifier to distinguish between normal process operation and fault situation and to precisely locate and diagnose the actual fault. Depending on the severity and security relevance of the fault, the FDS causes appropriate actions. FDS structure is depicted in Fig. 33 [7].

All faults occur in, or are at least associated with, a particular component or subsystem. For each component, therefore, we attempt to identify all possible faults or other abnormal conditions. These are divided into three categories, *cautions*, *warnings* and *alarms*, which indicate different levels of urgency and initiate different system responses [45].

A *caution* indicates that a particular monitored quantity is outside of its normal operating range and indicates a need for service and/or adjustment of the affected component. The system does not respond to a caution other than to annunciate the condition on the operator interface. It is up to the operator and/or service personnel to investigate the condition and determine if any special action is warranted. Cautions are annunciating on the operator touch screen by blue indicator lights.

A *warning* indicates that a particular monitored quantity is outside of acceptable operating limits. Continued operation at such levels could lead to component damage and/or power system failure. The system responds to a warning by performing a controlled shutdown of the affected component. If it is a power-generating component, sufficient replacement generating capacity is

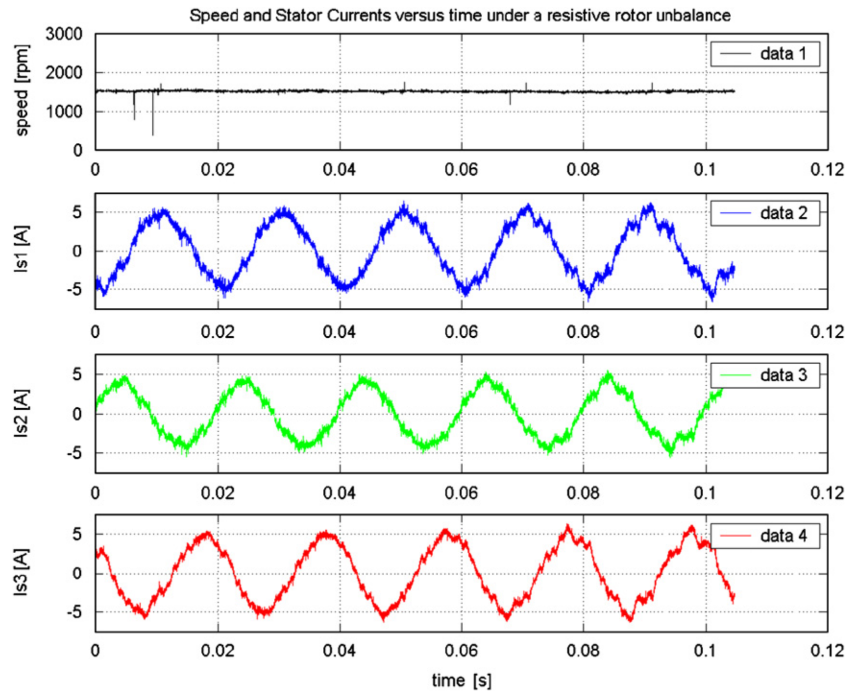


Fig. 32. The rotor speed and stator currents of DFIG acquired by ICS-645 under the resistive unbalance of 1.2 Ω in one rotor phase at 2 kW.

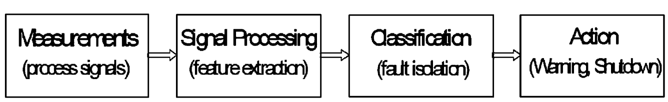


Fig. 33. Structure of a fault detection system.

brought on-line before the component is taken off-line. Warnings are annunciated on the operator touch screen by yellow indicator lights.

An *alarm* indicates a severe malfunction that poses an immediate danger to personnel and/or equipment. The system responds by immediately disconnecting and shutting down the affected component without regard for the ability of the remaining components to meet the primary load. An alarm condition is by definition sufficiently serious that it is preferable to risk a power outage than to allow the component to remain on-line. The affected component becomes unavailable and remains so until the precipitating condition is removed and the alarm cleared. Alarms are annunciated on the operator touch screen by red indicator lights.

3.2. Methodology

Numbers of techniques are available for identification of faults and these are listed below and line diagram of each approach is shown in Fig. 34 [7].

(i) *System identification approach*: This is a model-based approach uses system identification techniques (Fig. 34a). The input–output measurements are being conducted and then compared with the set values. The difference with set values shows the fault indicator through error signal.

Parameter estimation methods are well established and widely used in control systems, e.g., in adaptive controllers. They have also been successfully applied to a variety of fault detection problems where sufficiently accurate linear process models could be derived [46,47].

(ii) *Observer-based approach*: Methods based on state observers and Kalman filters are still a topic of active research. In this approach, the residual is the observation error—or innovative in case of the Kalman filter—calculated from the process measurements and the output of a reference model (Fig. 34b). The observer can be designed with reduced sensitivity against model uncertainties and structural external disturbances, but still very accurate models for the essential process dynamics are required. Only few industrial applications have been reported yet [48,49].

(iii) *Signal analysis approach*: Fault detection methods based on time- and frequency-domain signal analysis without explicit mathematical model are state of the art in process supervision (Fig. 34c). In this approach fault indicators are derived from process measurements via limit and trend checking of the process signals and by means of various spectral analysis method, e.g., Cepstrum, envelope curve analysis [50,51]. Especially with rotating machines (turbines, electrical machines, gearboxes, bearings) spectral

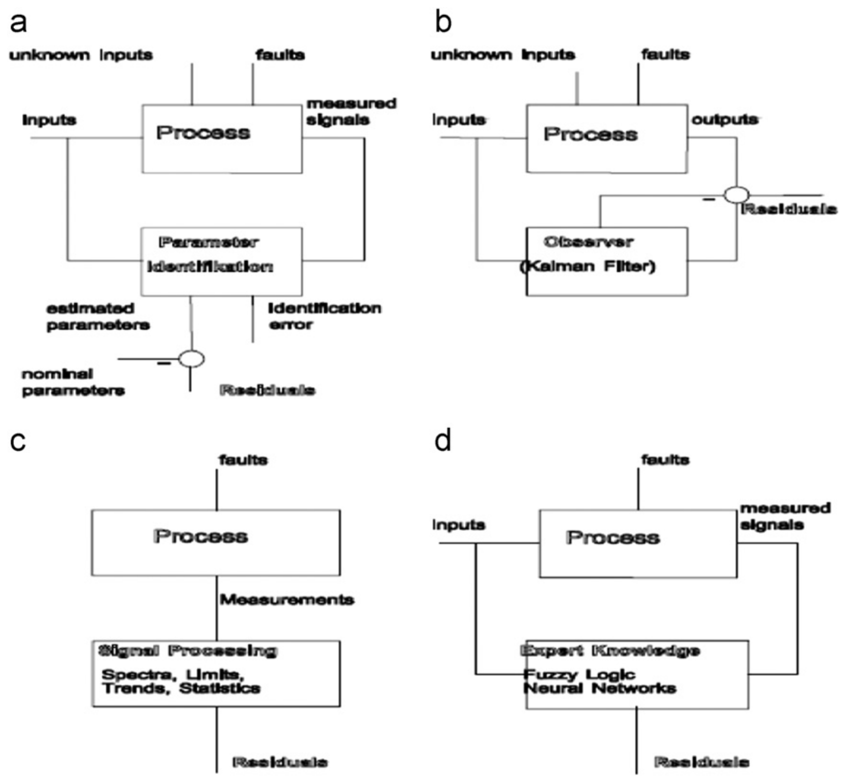


Fig. 34. Approaches to fault detection.

analysis has been successfully applied to yield detailed diagnosis and remaining lifetime estimates. Signal analysis methods will in general not be as fast as model-based approaches in detecting abrupt changes. But they can be applied to very complex systems and they do not require knowledge of input signals [7].

(iv) *Expert system and artificial intelligence (AI) approaches*: When a process is too complex to be modeled analytically, qualitative (expert) process knowledge can be used to evaluate relations between measured signals and current operating conditions (Fig. 34d). Also fuzzy techniques have been investigated in this context [52]. In some applications, Neural Networks have been used to substitute analytical process models. With a Neural Network that was trained on a reference process (e.g., the new machines) residuals can be generated similar to the model-based approaches [53]. While expert systems are quite common in FDSs [54]. Fuzzy and Neural Network approaches are still under research [7].

3.3. Algorithms

Different algorithms are developed for the detection of faults on the basis of different techniques. Each technique has certain advantages over other ones in reliability, simplicity, responsiveness and effectiveness. Algorithms are being made to detect the faults in components and may vary on the basis of component working principle, characteristics and criticality like rotor may have different algorithm from gearbox.

3.3.1. Global FDS

Methodologies are developed for fault detection, which can be applied on any subsystem, subassembly, or component. The need is to manipulate the formulae according the selected portion of system or on the whole system. The advantages are that with one approach you can detect fault and there is no need to apply separate method for each component in a subsystem or subassembly for fault detection.

Some of the approaches are summarized below which can be applied on any subsystem or subassembly of the WEC for fault detection and then in certain cases fault isolation.

3.3.1.1. Artificial intelligence. The community who is studying fault diagnosis on the basis of AI is also known as Diagnostic (DX) community.

The general objective of AI is to reproduce human reasoning and more generally any human cognitive mode of comprehension, perception, representation and decision making, as faithfully as possible [55]. There are two kinds of reasoning for solving diagnostic tasks:

normal-operation-oriented reasoning and abnormal-operation-oriented or abductive reasoning. Normal-operation-oriented diagnosis uses knowledge about how normal components work to detect deviations from normality in observed behavior, from which a minimal set of faults is hypothesized. Abnormal-operation-oriented diagnosis uses knowledge about how the components are affected by some specific faults in order to trace those faults [56]. Struss [57] emphasizes many advantages of AI model-based diagnosis, such as the possibilities of explicit conceptual modeling, automated model composition and structural model revision.

In the consistency-based approach [58], the description of the behavior of the system is component-oriented and rests on first-order logic. The {SD (system description), COMP (components)} pair constitutes the model. The system description takes the form of logical operations [59]. The extension of the predicate $ab(\cdot)$ represents the set of abnormal components.

Let OBS be the set of observations. Diagnostic reasoning has been summarized in the following way [60]. A diagnosis is a minimal set $\Delta \subset \mathrm{COMP}$ of abnormal components such that $\left\{ab(c) : c \in \Delta\right\} \cup \left\{-ab(c) : c \in \mathrm{COMP}\backslash\Delta\right\} \cup \mathrm{SD} \cup \mathrm{OBS}$, is consistent. Δ is minimal if no subset $\Delta' \subset \Delta$ is a diagnosis.

The diagnosis relies on the conflict notion: a conflict is a set of components $C \subset \mathrm{COMP}$ such that $\mathrm{SD} \cup \mathrm{OBS} \cup \left\{-ab(c) : c \in C\right\}$ is inconsistent; the observations indicate that at least one of its components must behave abnormally. A diagnosis is thus a set Δ of components such that $\mathrm{COMP}\backslash\Delta$ is not a conflict. The diagnosis proceeds in two steps: the first step determines the set of conflict sets C; the second step computes diagnoses from the conflict sets, using hitting sets: $H \subseteq \cup_{C \in C} C$such that $H \cap C \neq 0$ for any C in C. Reiter [58] has shown that $\Delta \subset \mathrm{COMP}$ is a minimal diagnosis for {SD COMP OBS} if and only if Δ is a minimal hitting set for the collection of conflict sets C.

Diagnosis in this framework is logically sound but a major drawback is the issue of combinatorial explosion for systems involving many components [61], as in the case of industrial processes [55].

3.3.1.2. FDI (fault detection and isolation). The FDI community is especially concerned with industrial process modeling and control. Models are quantitative and dynamic [62]. Two basic representations can be used: state space models and input–output relations. Eq. (8) is an example of an input–output relation, which takes into consideration the way faults and unknown disturbances d affect the measurable output y of the system, excited by an input u

$$y = h(u, f, d, t), \tag{8}$$

where y and u represent observations (OBS). Disturbances are uncontrolled input signals whose presence is undesired but normal (such as the wind for a plane or a resistive torque for a motor) and must be distinguished from faults. Noise is a special kind of disturbance related to random uncertainty. Faults are deviations from normal behavior in the plant or its instrumentation. Additive process faults are unknown inputs acting on the plant, which are normally zero. Multiplicative process faults lead to changes in model parameters. Sensor and actuator faults are other significant types of faults, represented as additive signals. A model (8) can take into account both additive faults (extra signals) and modifications to the model parameters (change in h) [55].

The model is used to compute numerical fault indicators, known as residuals T_j, which are null when there is no fault affecting the system. Residual generation refers to the elaboration of relevant fault indicators and has received much attention within the FDI community. It is worth noting that a residual, by using appropriate filters, can represent a much more elaborate quantity than a simple comparison of a process measurement with its model prediction [63].

3.3.1.3. Recursive isolation. Reasoning (DX) and computing (FDI) may thus be considered in opposition. The combined method (Recursive Isolation Algorithm) brings them together. It relies on both a qualitative causal representation of the process and on quantitative local models. It has been inspired by AI for the causal modeling of physical systems and for studying logical soundness. But it takes advantage of control theory at the level of each elementary submodel to check local consistency. Process dynamics are taken into account using relations between variables that manage time explicitly [55].

It is applied each time new data are acquired on the system to be diagnosed. The interest of recursive isolation is to prevent combinatorial explosion. The objective of causal diagnosis is to search for the source node(s) whose state(s) explain all the observed deviations in the graph. Once a source node is found, it has to be interpreted in terms of possible faulty components. The set of components Up_i, IS_i and Loc_i are thus defined in following equations:

$$\mathrm{Up}_i = \mathrm{Upstream}\,(Y_i^*, 0), \tag{9}$$

$$\mathrm{IS}_i = \bigcup_{Y*(j) \in U_i^*} S(j), \tag{10}$$

$$\mathrm{Loc}_i = \mathrm{Local}\,(Y_i^*, 0), \tag{11}$$

Up_i and Loc_i, respectively, refer to upstream and local components with respect to node $Y_i^* = Y^*(i)$ is the set of sensors related to U_i^*, the measured input nodes of the local subgraph related to Y_i^*. Introducing such partitions within the components in COMP will be shown to be relevant in order to implement recursive isolation [55].

Tables 4–6 are containing information about the isolation properties of residuals, isolation level and algorithm path, respectively (Table 7).

The proposed algorithm enables on-line determination and evaluation only of the residuals required for fault

isolation reasoning. That is an important difference with the FDI approach, where the size of the signature vector is fixed a priori: all the address range registers (ARRs) have to be evaluated at each measurement acquisition step. Another important difference is that the causal diagnostic algorithm does not require any assumption about the way single fault effects may be combined to tackle the multiple fault case [55].

3.3.2. FDS of subsystem

3.3.2.1. Rotor. *Transmittance functions (TF)* [64]: The technique is specialized for use with a laser vibrometer, which measures structural velocities. An integral damage indicator between degree of freedoms (DOFs) r and s is

$$d_{rs} = \int_{f1}^{f2} (T_{rs}^{\mathrm{h}} - T_{rs}^{\mathrm{d}})\,\mathrm{d}f \bigg/ \int_{f1}^{f2} (T_{rs}^{\mathrm{h}})\,\mathrm{d}f, \tag{12}$$

$$T_{rs} = \frac{h_{r0}}{h_{s0}} = \frac{v_r/f_0}{v_s/f_0}, \tag{13}$$

where superscripts h and d in Eq. (12) represent healthy and damaged structure. The quantities $h_{r0} = v_r/f_0$ and $h_{s0} = v_s/f_0$ are the mobility frequency response functions (FRFs) computed by the scanning laser doppler vibrometer (SLDV), shown in Fig. 35, for forces of magnitude f_0 acting simultaneously at DOFs defined are by the k vector and TF is computed using the laser data in Eq. (13).

An advantage of using TFs is that the excitation force is cancelled and does not need to be measured if it is equal in amplitude at all points where applied. In addition, the ratio of responses partially cancels changes in the TFs due to environmental effects such as temperature changes. Since TFs are ratios of two continuous functions with peaks and valleys, they are quite sensitive to shifts in frequencies or damping caused by damage. Healthy and damage portions are shown in Fig. 36.

The experiment has shown that the TF method is sensitive to damage as well as noise in the measurements. The indication of damage is clear but the location is not always correct. A finer resolution grid would improve locating damage.

Operational deflection shapes (ODSs) [64]: ODSs are computed by the SLDV system for the healthy and damaged structures. Changes in the ODSs are used to indicate and possibly locate damage.

The ODS are given by

$$x\left(\frac{\theta_m}{\omega_{\mathrm{dr}}}\right) = \mathrm{Re}\left[X(\mathrm{j}\omega_{\mathrm{dr}})\mathrm{e}^{\mathrm{j}\theta_m}\right]. \tag{14}$$

Table 5
Isolation properties of the residual tests used in the recursive isolation algorithm

		Up_i		IS_i	Loc_i	
T_i^1				X	X	Step 1 : Detection and First isolation level
T_i^0		X		X		
...	X			(shaded)	(shaded)	Step 2 : Second isolation level (Selection of upstream paths + recursive calls)
T_i^m		X		(shaded)	(shaded)	
...			X	(shaded)	(shaded)	

Table 6
First isolation level: local diagnosis reasoning

Tests value	(Local) minimal diagnosis
$(T_{-i}^0, T_i^1) = (0,0)$	{ }(*no fault detected*)
$(T_{-i}^0, T_i^1) = (0,1)$	{{IS_i}, {Loc_i}}
$(T_{-i}^0, T_i^1) = (1,0)$	{{Up_i}, {IS_i}}
$(T_{-i}^0, T_i^1) = (1,1)$	{{IS_i}, {Up_i, Loc_i}}

Table 7
Algorithm for path selection and recursive calls

```
For j = 1...card(U_i^0)
  m = [1...1]
  m(j) = 0   /* Select the j^th propagation path with */
  If T_{-i}^m = 1 Then
     /* The node U_i^*(j) is suspected; it belongs to the
        propagation path of the deviations: recursive call */
      Go to Step 1 with Y_i^* = U_i^*(j)
     Else
        /* Search for the source not pursued in the upstream
          Direction with respect to U_i(j) : local exoneration */
     End if
  End for
```

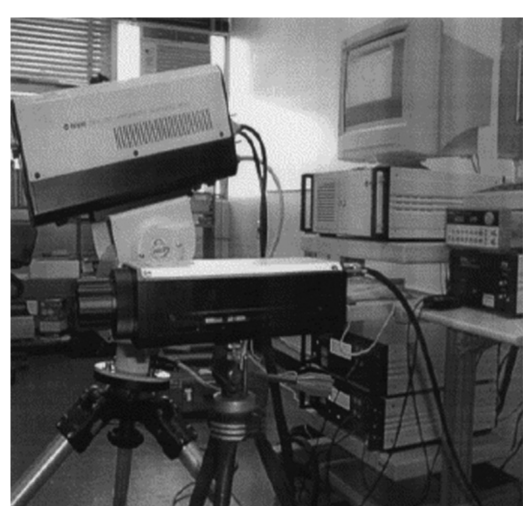


Fig. 35. Scanning laser doppler vibrometer system.

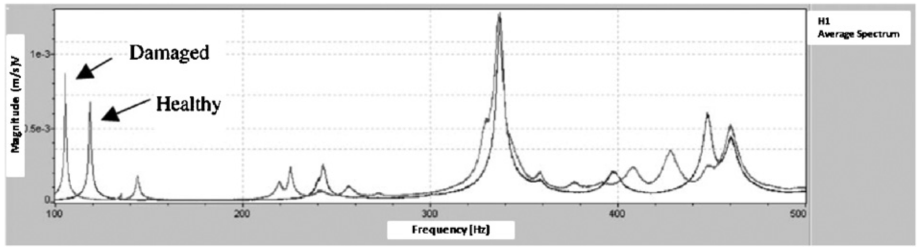


Fig. 36. FRF comparison of the damaged and healthy structure in the frequency range 100–500 Hz.

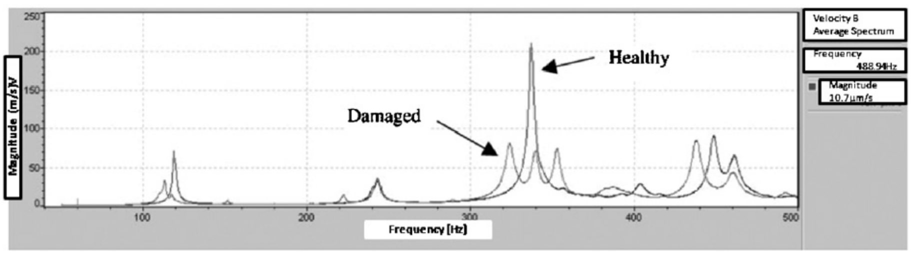


Fig. 37. Averaged spectra for the ODS test, 0–500 Hz.

For velocities

$$v\left(\frac{\theta_m}{\omega_{\mathrm{dr}}}\right) = \mathrm{Re}\left[\mathrm{j}\omega_{\mathrm{dr}}X(\mathrm{j}\omega_{\mathrm{dr}})\mathrm{e}^{\mathrm{j}\theta_m}\right], \tag{15}$$

where ω_{dr} is one specific driving or excitation frequency. The ODS can be evaluated at specified angles, $\theta_m = 2\pi\, m/p$ where p is the number of points in one cycle of vibration to evaluate the ODS, and $m = 0, 1, 2, p-1$, Re is real part, $\mathrm{j} = \sqrt{-1}$, x and v are representing displacement and velocity, respectively.

The SLDV uses a periodic chirp excitation and the vibration response is measured for one period of the excitation. A Fourier transform is performed and the complex vibration response at the particular measurement point is stored. This is repeated for all scan points and the real amplitudes are plotted at selected phase angles. This is called the ODS and approximately coincides with the more familiar mode shape if the mode shapes of the structure are well spaced, damping is small, and the excitation is at a natural frequency of vibration of the structure. The ODS may be more accurate at detecting damage because the exact response of the structure is used, subject only to errors in performing the Fourier transform (Fig. 37). Mode shapes, however, involve additional assumptions and procedures to compute which may remove some of the effects of damage to a structure.

Resonant comparison [64]: It can be used with a small number of PZT patches as sensors to accurately detect damage in critical areas of the structure. Localized symmetrical properties of the structure are exploited in this approach to minimize the need for pre-damage data and to compensate for changes in the structure not related to damage. Damage is determined using the differences in the response at the resonances of the healthy and damaged structure. It is defined as

$$d_{ij} = \Delta^{\mathrm{d}}_{ij} - \Delta^{\mathrm{h}}_{ij}, \tag{16}$$

where $\Delta^{\mathrm{d}}_{ij} = \max|(\varepsilon d_i - \varepsilon d_j)/f|, \Delta^{\mathrm{h}}_{ij} = \max|(\varepsilon h_i - \varepsilon h_j)/f|$, ε is the strain measured at point i or j, the superscripts on Δ_{ij} denote damaged (d) or healthy (h), and f is excitation force amplitude. For symmetric structures, ${\Delta^{\mathrm{h}}}_{ij} \approx 0$.

Signal responses of healthy and damage conditions are depicted in Fig. 38.

Wave propagation [64]: It can be used with a small number of PZT patches as sensors to accurately detect damage in critical areas of the structure. Damage is determined using the differences in the time impulse response of the healthy minus the damaged structure. It is defined as

$$d_{ij} = \frac{1}{Tf}\int_0^T \left|\varepsilon^{\mathrm{d}}_{ij} - \varepsilon^{\mathrm{h}}_{ij}\right| \mathrm{d}t, \tag{17}$$

where ε is the strain measured at point i or due to an impulse at point j, the superscripts denote damaged (d) or healthy (h), T is the time of integration, and f is excitation force amplitude.

In Fig. 39a the input impulse is shown which is 45 V peak with approximate half-sine duration of one thousandth of one second. The response for patch 3 is shown in the healthy case in Fig. 39b, the damaged case in Fig. 39c, and the difference in the healthy and damaged responses in Fig. 39d. The magnitude of the scale in Fig. 39(d) is 10 times smaller than in Fig. 39(b) and (c) to show the detail of the difference. The damage is a $2 \times 15/16'' \times 2 \times 15/16'' \times 5/18''$ steel plate clamped onto the back lower left end of the blade. Since this damage is not located between the

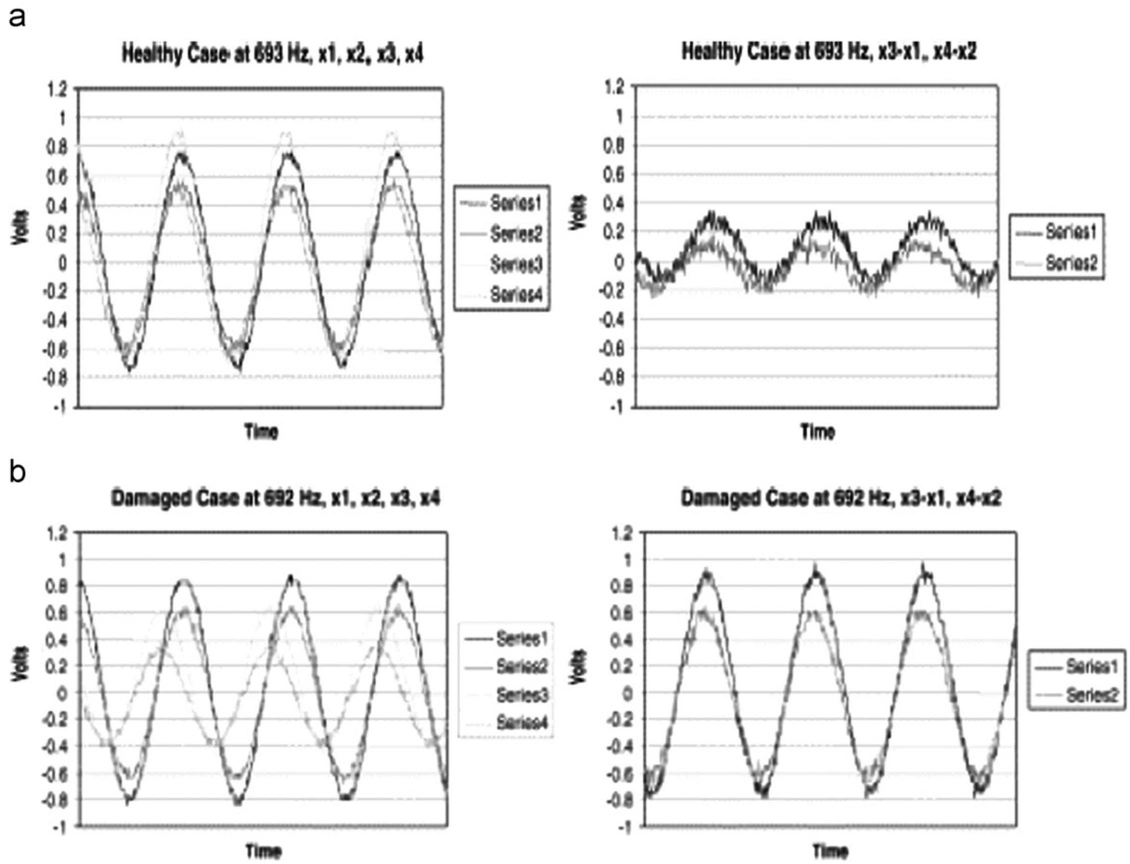


Fig. 38. (a) RC sensor responses for healthy case at ~693 Hz (left) and non-symmetry values $|x3-x1| = 0.3$, $|x4-x2| = 0.2$ (right) and (b) RC sensor responses for damaged case at ~692 Hz (left) and damage values $|x3-x1| = 0.9$, $|x4-x2| = 0.6$ (right).

actuator and the sensor, the change in wave propagation is small. The trailing part of the impulse response is changed the most due to the damage.

Variance analysis [65]: The variance damage index "d_i" is used to quantify the damage detected at the ith sensor. This is computed as the square of the healthy, minus damaged vibration signals, normalized by the variance of the healthy signal (assuming the mean is zero). The damage indicator is computed as

$$d_i = \frac{\int_{r_1}^{r_2} \left[x_i^{\mathrm{h}}(t) - x_i^{\mathrm{d}}(t)\right]^2 \mathrm{d}t}{\int_{r_1}^{r_2} \left[x_i^{\mathrm{h}}(t)\right]^2 \mathrm{d}t}, \tag{18}$$

where $x_i^{\mathrm{h}}(t)$ is the voltage from the PZT i in the healthy case, the superscript h is the response from the healthy structure, d is damaged and t is time.

The variance damage indicator is computed for the four sensors and the result is plotted in Fig. 40. The sensors located farther from the fixed end of blade have greater response due to the flexibility of blades at free end. As the load increases, the receiver responses R1 and R2 diverge while the sensor responses R3 and R4 stay close together. The sensor responses R3 and R4 cross and drop below the response of R2 when the level reaches above approximately 3300 lbs (146,79.13 N). The receiver responses R1 and R2 diverge because damage is occurring between them. The responses from receivers R2, R3 and R4 are similar because they are on one side of the damage area while the receiver R1 is on the other side of the damage area. The effect of compressive and buckling loading on the propagation of stress waves in a composite shell structure is unknown. The flat composite plates be tested in a material testing system (MTS) machine under compressive buckling loading. Stress waves can then be propagated in the plate to failure. This would provide a better understanding of damage propagation and allow the health-monitoring sensor system to be optimized to sense this type of damage.

Wavelet pattern recognition analysis [65]: Wavelet analysis, which is a linear transformation, is able to resolve time dependent variations without interference. An infinite number of different wavelets within both discrete and continuous wavelets classes raise the important question of which wavelets to choose for a specific signal. The most appropriate wavelets to use for damage detection are a topic currently under investigation. Some guidance based on regularity, vanishing moments and time–frequency localization of wavelets can be considered. In general, continuous wavelets are better for time-frequency analysis while discrete wavelets are more suitable for decomposition, compression and feature selection.

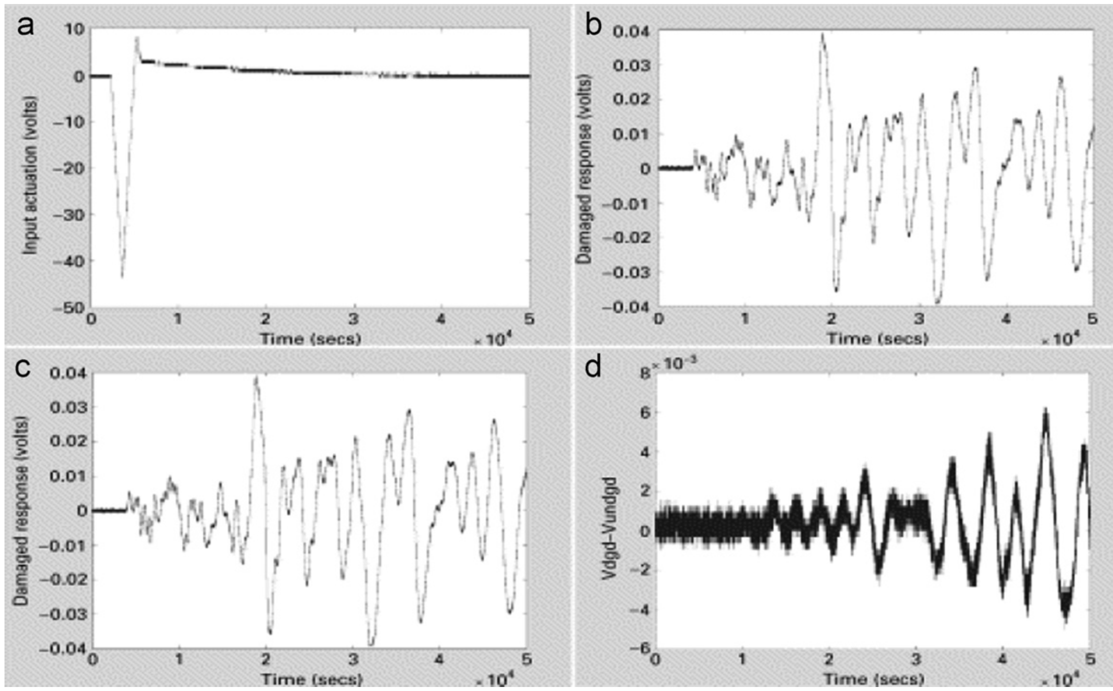


Fig. 39. Input and response for the wave propagation method (a) input pulse, (b) healthy response, (c) damaged response, and (d) healthy-damaged response. The added steel plate (2 × 15/16″ × 2 × 15/16″ × 5/16″) was placed away from the linear path between the actuator and the sensor. The change in the trailing part of the Impulse Response indicates damage.

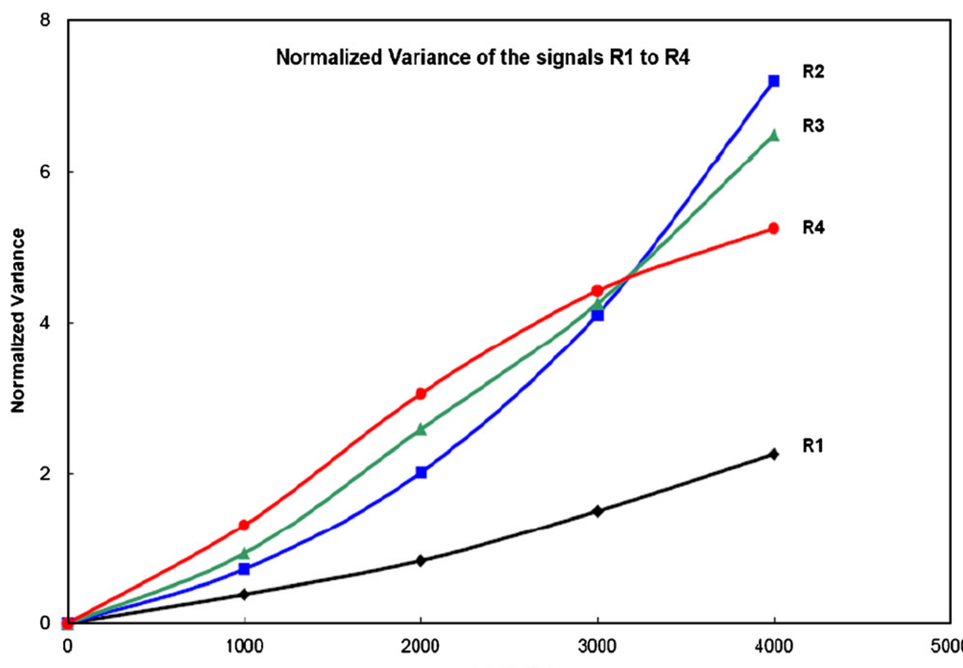


Fig. 40. Variance damage indicator for each sensor.

The Mexican Hat wavelet is used to detect damage in the blade. This wavelet function (Fig. 41) is derived from a function that is proportional to the second derivative of the Gaussian probability density function. The excitation or reference signal at transmitter T1, and the resultant stress wave signals from sensor R1 at the no load, and 4000-lb (192,97.6 N) load conditions are shown in Fig. 41. The wavelet transform is first performed on the excitation signal for reference and for understanding the characteristics of the transform (Fig. 42). The wavelet

transformation is then performed on the response R1 signal in the no load condition (Fig. 43, left), to be used as the healthy or historical pattern, and for the response R1 signal at the 4000-lb (192,97.6 N) load condition (Fig. 43, right). A comparison of the wavelet maps for the response

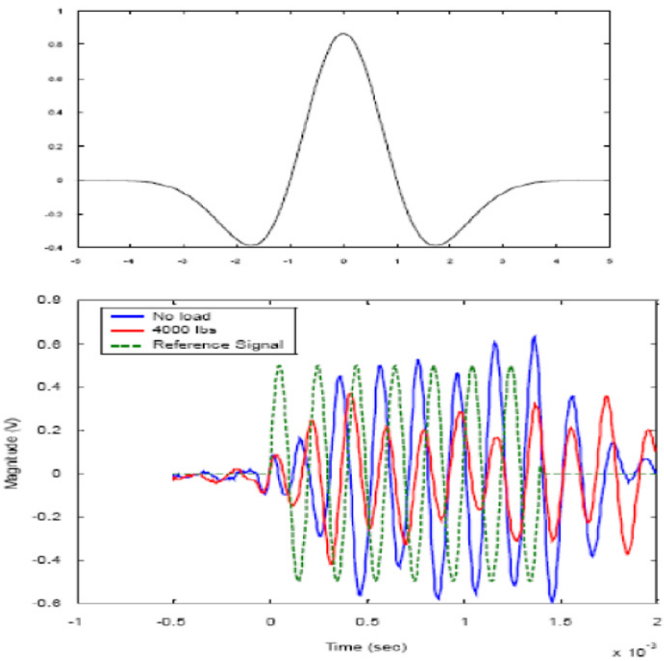


Fig. 41. The excitation or reference signal at transmitter T1 and resultant stress wave signals from sensor R1 ate no load & 4000-lb load conditions.

R1 in the healthy and loaded condition show a difference in patterns. This difference indicates a change in the blade structural properties or damage. A more quantitative means of classifying the damage using wavelets is being investigated.

Thermoelastic (TE) stress analysis [66]: The TE equipment is a Deltatherm 1000 TE stress measurement system [67]. The equipment consists of a set of infra-red detectors arranged in a focal-plane array and represents a major improvement on the previous generation of thermoelastic stress analysis (TSA) systems, known as stress pattern analysis by thermal emission (SPATE), which relied on a single sensor scanning across the surface, since full-field measurements can be made in a few seconds, compared to several hours with SPATE. Practically simultaneous temperature measurements can also be taken using the Deltatherm. Due to the high temperature sensitivity of the Deltatherm infrared sensor material and the low thermal conductivity and diffusivity of the glass/polyester blade material, TE stress measurements of the blade surface are sensitive to spatial and temporal temperature variations. For this reason it is necessary to keep the load amplitude to a minimum during the TE measurement campaigns.

TSA is applied during the blade fatigue test and to detect two deliberate flaws inserted into the blade during manufacture, namely a shear web disbond in the main structural spar and a trailing-edge delamination in the maximum chord region between 900 and 1100 mm (Total blade length is 4500 mm). The sinusoidal, constant amplitude fatigue loading is applied via a wooden saddle

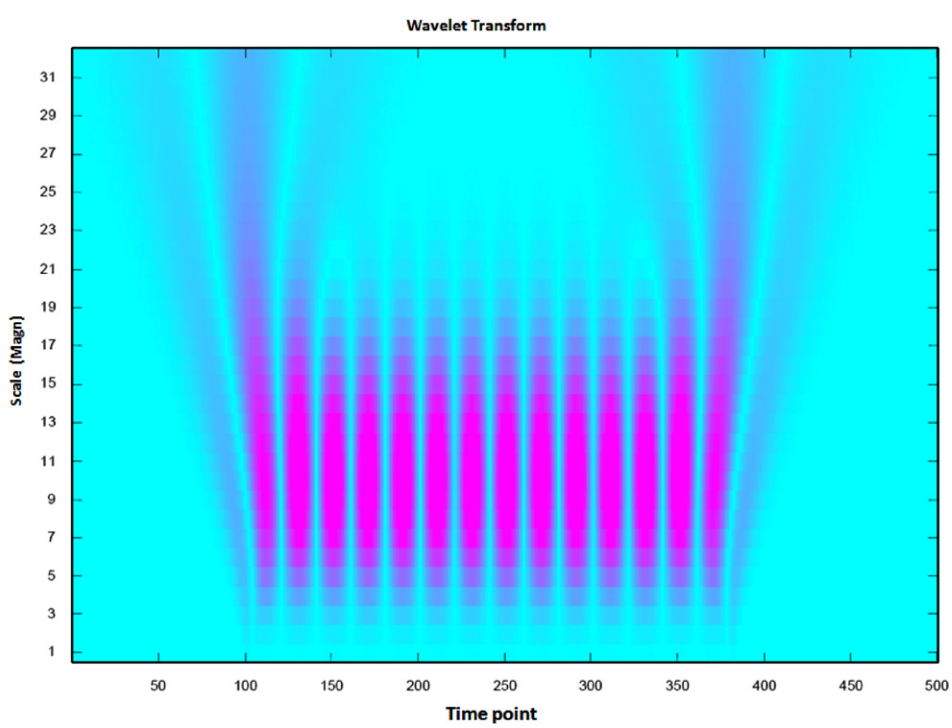


Fig. 42. Wavelet transform of the excitation sine burst signal.

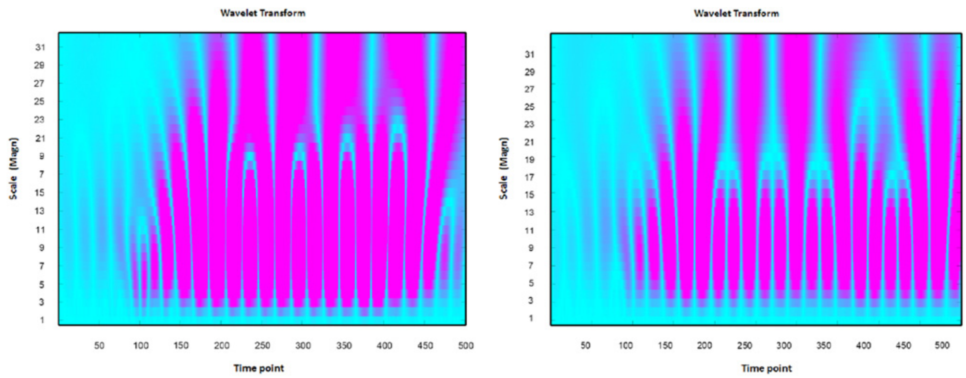


Fig. 43. (left) Wavelet transform of the response signal R1 at zero load, (right) Wavelet transform of the response signal R1 at 4000-lb load.

at 3000 mm from 0.3 to 3.0 kN during the TE stress measurement campaigns in order both to reduce the influence of physical blade movement on the readings and, in particular, to reduce viscoelastic heating effects in regions of high stress concentration The blade survived almost 4 million cycles.

A block diagram showing the main components of data collection and processing is shown in Fig. 44.

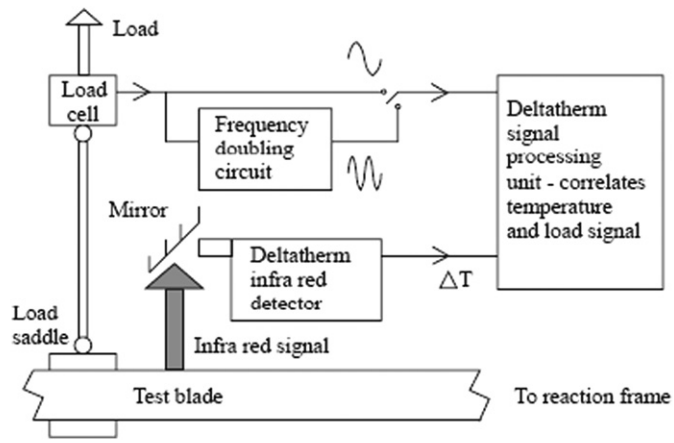


Fig. 44. Diagrammatic representation of thermoelastic data collection and load signal processing.

A software suite are written in Matlab to calibrate and post-process the data, including alignment of adjacent frames against an outline of the blade plan.

The trailing-edge flaw grew very early in the test and then stabilized, while the shear web disbond is visible right from the start as a TE stress ''hot'' spot (Fig. 45). Several further cracks initiated in the foam-filled trailing-edge part of the blade during the course of the test.

Fig. 46 shows the TE stress distribution measured shortly before final failure. The blade root is at the right of the picture and the leading edge at the base; the blade plan form can be easily distinguished. The picture is complicated by the ''noise'' of AE sensors arranged along the quarter-chord line and strain gauges and associated wiring. The main stress is carried by the spar along the leading edge. The outlined black rectangle to the middle-left of the picture encloses the foam-filled trailing-edge section in which three discrete cracks are visible (at 1570, 1850 and 2040 mm).

Close, visual inspection of the cracks in the trailing-edge sandwich part of the blade revealed flexing of the blade skin, as if local, small-scale buckling is taking place. These flexures appear to give rise to surface movements with a frequency higher than that of the test load. To test this hypothesis, a test signal is generated with twice the applied load frequency and correlated with the TSA signal. Surprisingly, this procedure is not only identified the cracked areas in the foam-filled sandwich area, but also successfully identified the root delaminations, and trailing-edge crack, and at the same time removed most of the signal noise.

The second harmonic TE stress plot for the blade (Fig. 47) successfully highlights all the damaged areas (dark features) and it can be argued further that the plot indicates the severity of damage at the (propagating) crack located at 2040 mm, since the signal strength is highest at this flaw. Further discussion of these results can be found in Paynter and Dutton [68].

3.3.2.2. Drive train. *Frequency analysis*: The fault detection is often based on frequency analysis and level detection for certain frequency bands, (see Fig. 48, source Prüftechnik). Based on the level of amplitudes, status signals can often be defined and generated. Diagnosis is often done by the supplier of the CMS or of the gearbox supplier. Specialized knowledge is required for signal interpretation. The effectiveness of these systems is becoming more evident for large-scale applications. Due to the non-stationary operation, it appears to be difficult to develop effective algorithms for early fault detection, especially for variable speed operation. Practical experience builds up very slowly, because component degeneration is fortunately a slow process and additional information about turbine loads and operational conditions are only fragmentarily available [17].

Artificial intelligence [69]: AI is now playing important role in the health monitoring and fault prediction scheme of WEC.

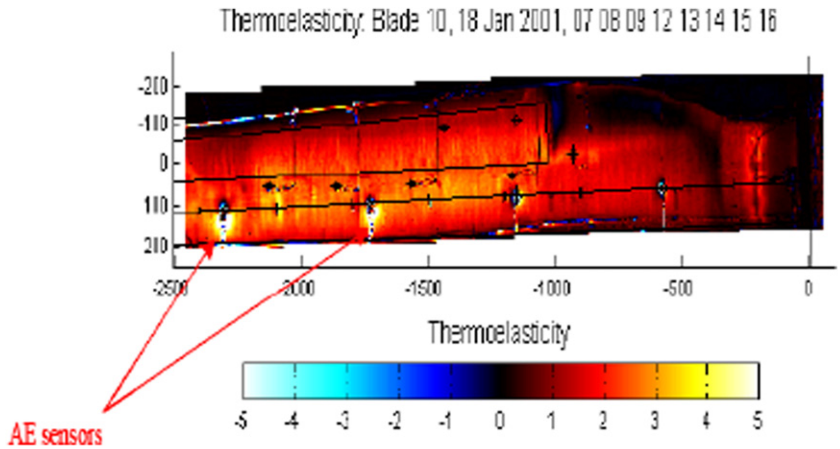


Fig. 45. Composite plot of normalized thermoelastic stress distribution on blade 10f near start of test.

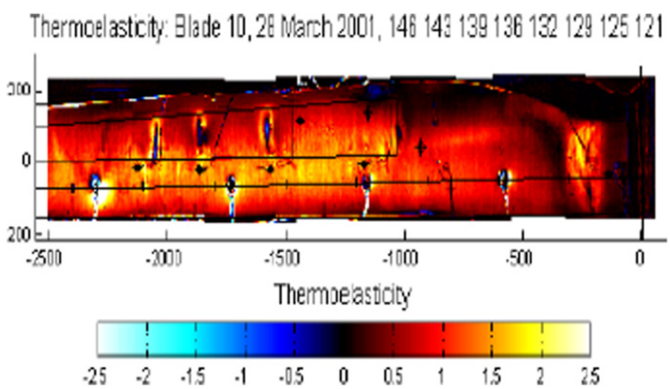


Fig. 46. Composite plot of normalized thermoelastic stress distribution on blade 10f near start of test showing cracks detected at locations 2040, 1850, 1570, 1220, and 1010 mm from the blade root and delamination in the root stock.

Intelligent system for predictive maintenance (SIMAP) is based on artificial intelligent techniques. The new and positive aspects of this predictive maintenance methodology have been tested in wind turbines. *SIMAP* is applied to a wind farm owned by a Spanish wind energy company called *Molinos del Ebro*, *S.A*.

The behavior and health condition of the wind turbine gearbox can be described by three characteristics: gearbox bearing temperature, cooling oil temperature of the gearbox and the difference between the hot and cold temperatures of the oil circulating through the gearbox cooling circuit. Normal behavior of these three parameters can be formulated by following the diagram given in Fig. 49.

Once the normal behavior models are obtained, it is possible to use them for the detection of possible anomalies and for refitting the maintenance planned according to the real health of the physical components. In order to do this, the input and output variables of the normal behavior models are taken in real-time and a prediction of the output is obtained in real-time too. The comparison between the values of the real and estimated output variables is used to detect possible anomalies to be diagnosed and to be mitigated by the corresponding maintenance action.

Fig. 50 shows a real evolution of the gearbox bearing temperature using the normal behavior model obtained by using Fig. 49. This figure covers a time period of 4 days (March 5–8 all inclusive). It is clear that around March 6, the real value of the bearing temperature is going outside the upper band of the normal value predicted for this temperature. The residual or difference between the real and estimated values of the bearing temperature is growing from March 6 on, but the gearbox is still working. Finally, on March 8 the gearbox fails and the wind turbine is unavailable to produce energy. Also, Fig. 50 demonstrates the ability of a normal behavior to detect anomalies before a catastrophic situation is present.

Similarly, the gearbox real and estimated thermal difference, and real and estimated cooling oil temperature models during the same period of time can be obtained as shown in Fig. 50 for gearbox bearing temperature.

The normal behavior models obtained are very useful for two different reasons. First, they can detect anomalies that do not correspond to normal behavior and that can evolve to catastrophic failures. Second, they can be used for a qualitative estimation of the health condition of a component based on the stress or residual obtained from the difference between real and estimated values. Both aspects can be used for re-planning the predictive maintenance according to the real situation of a component.

Torsional vibration (TV) [70]: If a crack develops in one of the gear teeth in the gearbox, it is anticipated that there will be minute variations in the shaft speed due to increased deflection of the cracked tooth as it comes into mesh. In order to determine the likely amplitude of these variations (and hence assess the ability of the TV diagnostic system to detect it) a simple model to estimate the speed variations is developed. Two gear teeth in mesh are shown in Fig. 51.

It is assumed that only two gear teeth are in contact at any given time. Deflection of the gear teeth in the tangential direction will lead to a degree of transmission

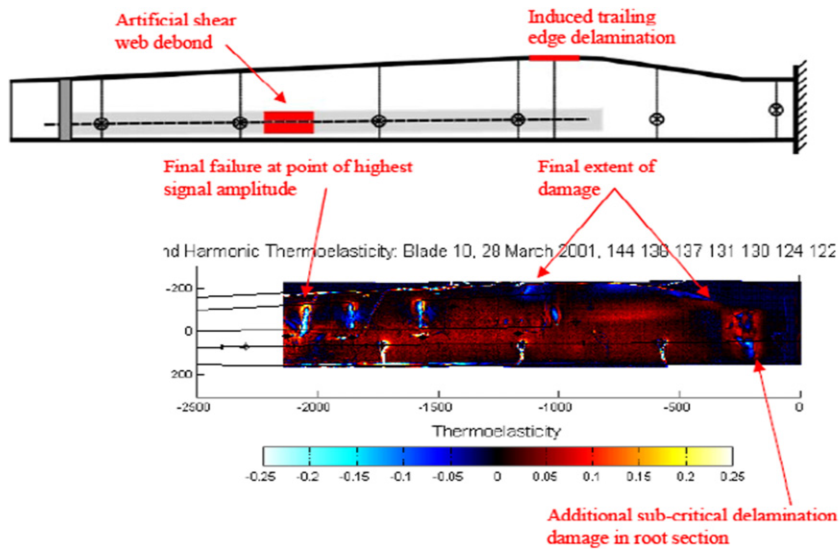


Fig. 47. Composite plot of second harmonic thermoelastic stress distribution on blade 10f near start of test showing cracks detected at locations 2040, 1850, 1570, 1220, and 1010 mm from the blade root, delamination in the root stock, and trailing-edge damage.

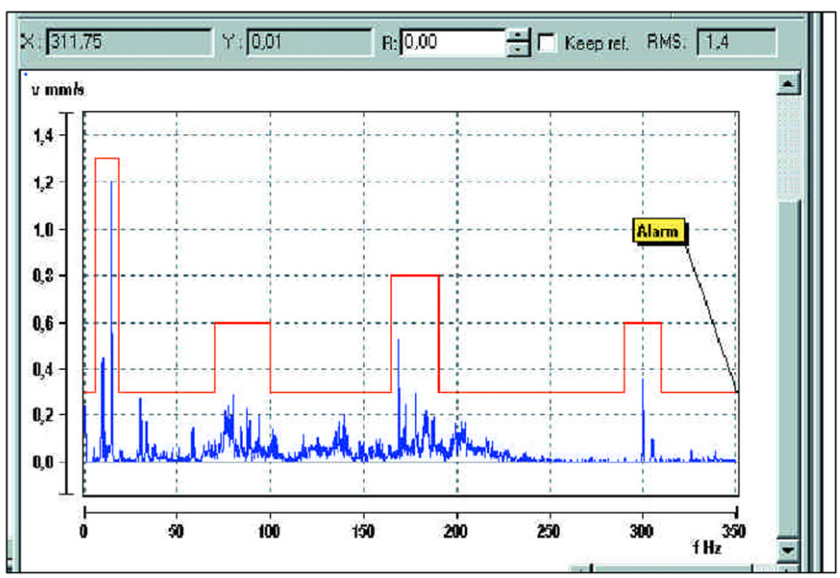


Fig. 48. Example of fault detection based on FFT (*Source*: Prüftechnik).

"error" which is defined here as the difference in angle between a perfect gear with completely rigid teeth and the actual gear with finite stiffness. The deflection of a single tooth is estimated by considering it as a cantilever with a point load halfway along its length.

Once the deflection of the gear tooth is known, the angular deflection/transmission error of the gear can be calculated.

The effect of a crack going right across the gear at the base of the tooth can be modeled. A crack at the base of the tooth will reduce the cross sectional area and hence the second moment of area at that point. For the sake of simplicity, the new I (second moment of area) value at the crack will be assumed to apply across the whole length of

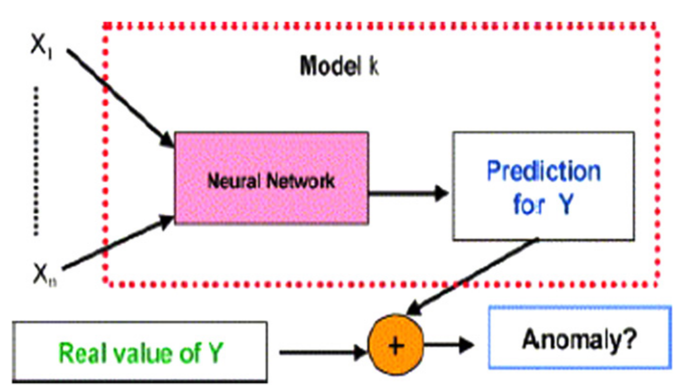


Fig. 49. Normal behavior model. Work scheme.

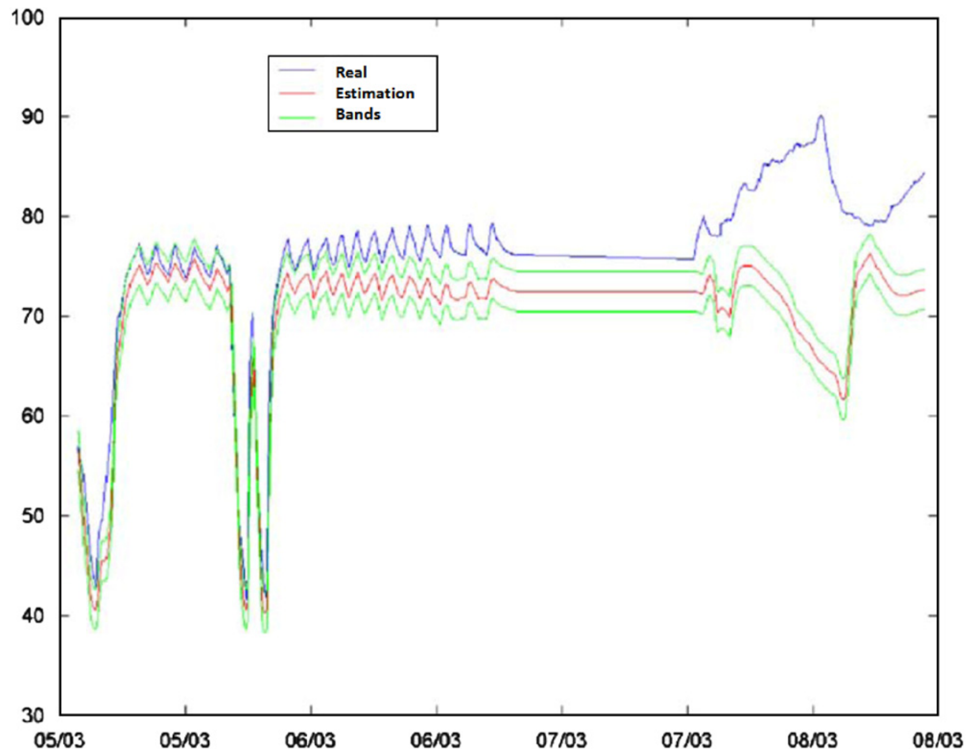


Fig. 50. Real and estimated gearbox bearing temperature when an anomaly is present.

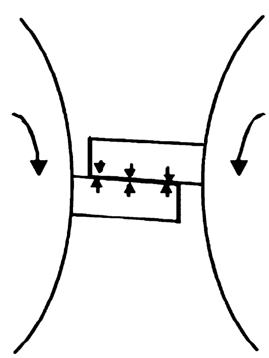


Fig. 51. Representation of two gear teeth in mesh.

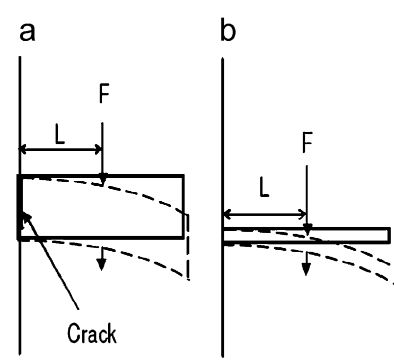


Fig. 52. Approach used to model crack at base of gear tooth.

the tooth—i.e., the behavior of the beam in Fig. 52(a) can be approximated by the beam in Fig. 52(b).

Using this simple model, a crack across 70% of the tooth is found to produce a deflection 37 times greater than that for an uncracked tooth. The speed fluctuation will decrease significantly with smaller cracks. Fig. 53 below plots the percentage speed fluctuation as a function of crack depth.

Using this model, a crack depth over 60% should be detectable. However, in making this assessment, the relative simplicity of the current model must be remembered.

3.3.2.3. Pitch mechanism. *FFT spectra analysis* [70]: The simulations have shown that the pitch error is best detected by the 1P-amplitude of the acceleration in the X- and Z-direction, where a difference of 3–4 dB between pitch error increments of 0.5° is observed. The amplitude separation is also observed in the electrical power signal and in the acceleration in the Y-direction, but it is less significant. Fig. 54 compares linear averaged FFT-spectra of in the X-direction for 4 different pitch errors.

Narrow band frequency spectra of the acceleration in the X-direction on the wind turbine's main bearing, shown for simulation of 4 different pitch errors applied on one rotor blade. The variation of the 1P component (approx. 0.43 Hz) is observed in the figure, 0–2 Hz, frequency resolution 0.024 Hz, time average over 300 s.

3.3.2.4. Yaw system [44]. The change in degrees of yaw gives the degree of fault like 5° (within normal operating range), 10° (unusual wind changes), and 20° (significant loads on wings).

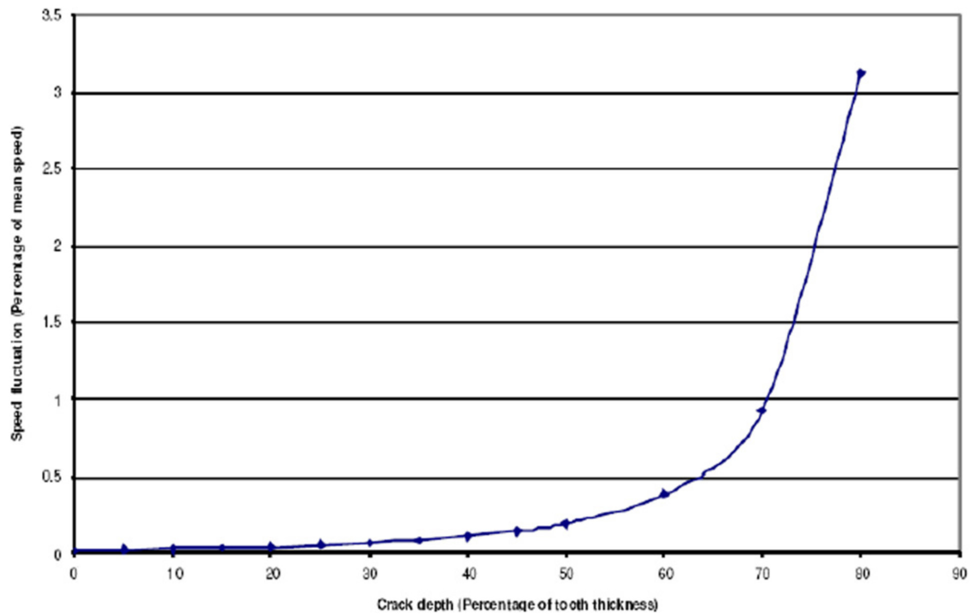


Fig. 53. Effect of crack depth on speed fluctuation.

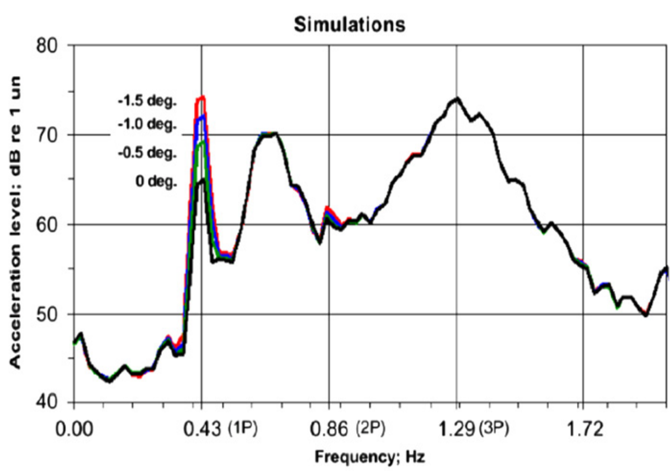


Fig. 54. Simulation of pitch errors.

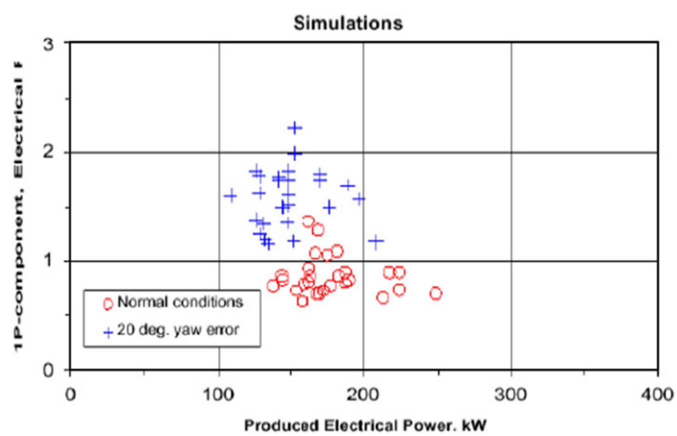


Fig. 55. Simulation of 1P component of a 20°. Yaw error compared to no yaw error.

The analysis of the yaw error simulations showed that the level at the 1P-frequency is altered by the amount of yaw error, as illustrated in Fig. 55.

This observation is important, as it will make it possible to distinguish between rotor blade pitch errors and rotor yaw errors, since only the latter has an influence on the1P-level of the electrical power. These relations have to be evaluated by the measurements in the test turbine. However, preliminary analysis of measurements with a stimulated yaw error, confirms the simulation results.

Plot of 10-s averages of the 1P-component of the electrical power, as function of the total produced electrical power is seen in Fig. 56. Comparison of measurements made in the test wind turbine at normal conditions and with a stimulated 20° yaw error. A clear separation of the data points is observed at powers above approx. 150 kW.

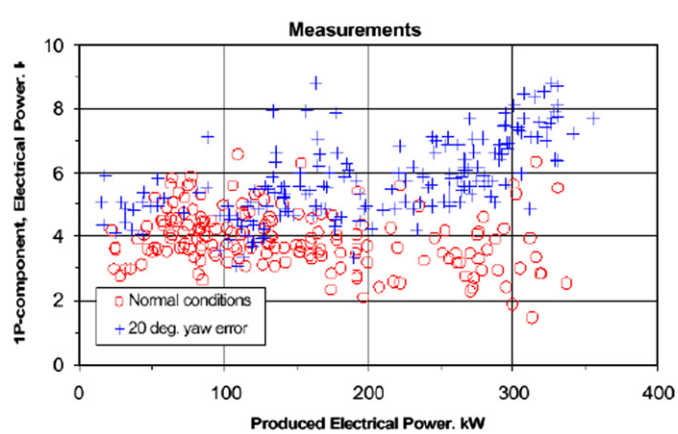


Fig. 56. Measurements of electrical power 1P components with 20° yaw and no yaw.

3.3.2.5. Electrical system. *Generator* [43]:

Machine current signature analysis (***MCSA***): Due to its powerful technique merits in diagnosis and detection of faults the MCSA monitoring technique can be chosen as a fault detection method.

MCSA to diagnose stator turn-to-turn faults: The objective of this method is to identify current components in the stator winding that are only a function of shorted turns and are not due to any other problem or mechanical drive characteristic. Eq. (19) gives the components in

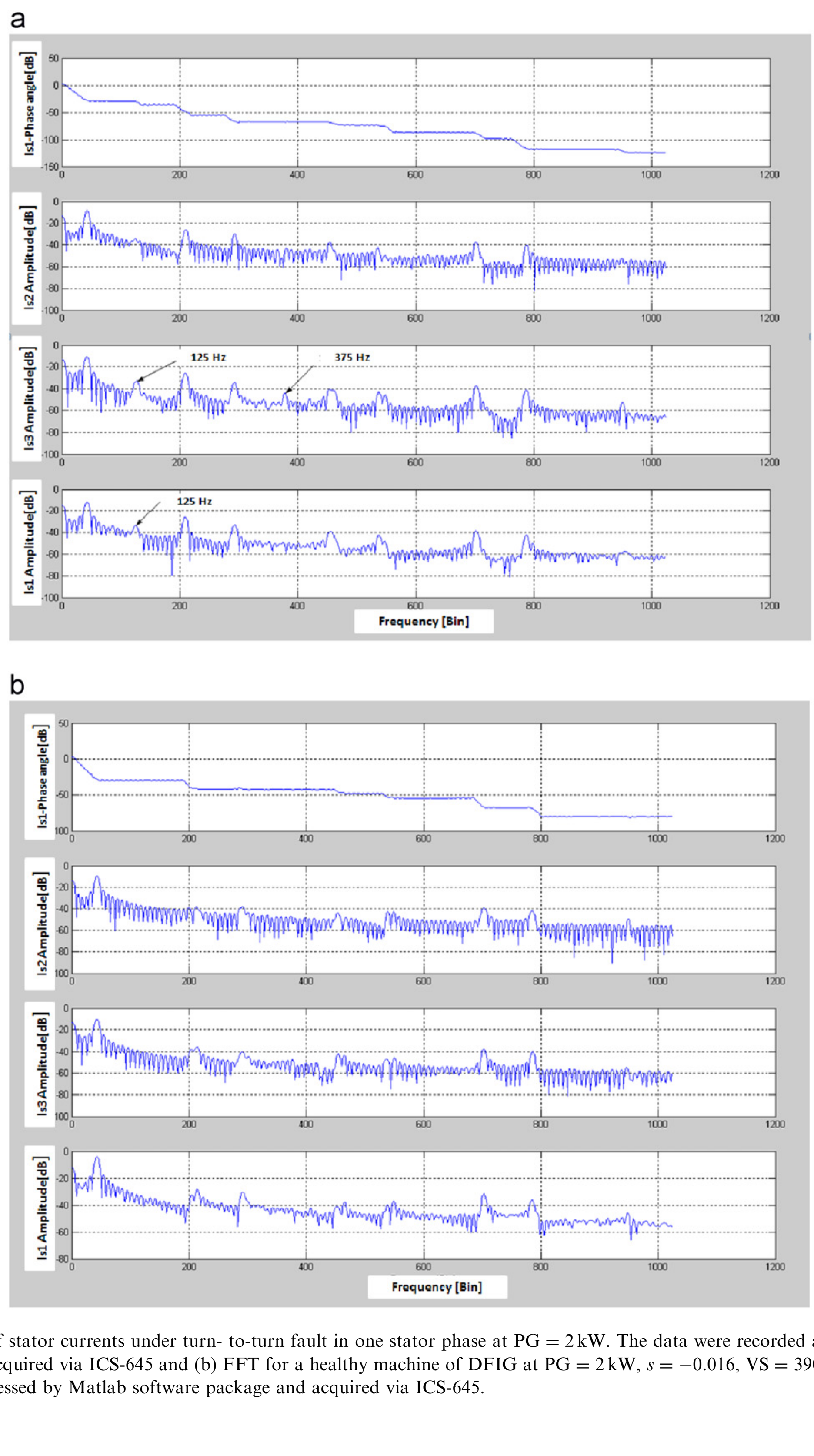


Fig. 57. (a) Spectrum of stator currents under turn- to-turn fault in one stator phase at PG = 2 kW. The data were recorded and processed by Matlab software package and acquired via ICS-645 and (b) FFT for a healthy machine of DFIG at PG = 2 kW, $s = -0.016$, VS = 390 V, IS = 4.7 A. The data were recorded and processed by Matlab software package and acquired via ICS-645.

the air-gap flux waveform that are a function of shorted turns.

$$f_{st} = f_1 \left[\frac{n}{p}(1-s) \pm k\right], \quad (19)$$

where f_{st} is the stator frequency components that are a function of shorted turns, f_1 is the supply frequency, $n = 1$, 2, 3… $k = 1$, 3,5,…p is the pole-pairs, s is the slip.

The diagnosis of shorted turns via MCSA is based on detecting the frequency components given by Eq. (19) in that these rotating flux waves can induce corresponding current components in the stator winding.

Fig. 57 gives the line current spectra for all stator phases under turn-to-turn fault (Fig. 57a) and with no stator fault (Fig. 57b). The obvious change, in Fig. 57a, is that completely new current components exist around 125 and 375 Hz and can only be due to the shorted turn, as per theory with $k = 1$, $n = 3$ and $k = 1$, $n = 13$ (Eq. (19)).

In addition, the Fig. 57(a,b) makes it clear that the difference between balanced operation and under turn-to-turn fault cases follow the phase angle of stator current-Is1. For instance the phase angle is changed around 125 Hz where a new faulty component exist as well.

Similarly using MCSA, faults in stator and rotor winding unbalances can be detected.

Transformer, contacting faults and switching gear: Thermography is a good tool to detect faults in transformer, contacting points and switching gears. For all these three components, this technique is described briefly.

Thermography: Thermography is often applied for monitoring and failure identification of electronic and electric components. Hot spots, due to degeneration of components or bad contact can be identified in a simple and fast manner. The technique is only applied for of line usage and interpretation of the results is always visual. At this moment the technique is not interesting for on-line condition monitoring. However, cameras and diagnostic software are entering the markets, which are suitable for on-line process monitoring. On the longer term, this might be interesting for the generator and power electronics [17].

Transformer: Thermography can be used for detecting of wiring and contacting faults on the transformers. It can also be useful for detecting winding problems, which lead to inhomogeneous temperature deviations in the phase windings. Fig. 58 shows a thermograph image of a 3-phase transformer. In the image, no significant differences in the temperature can be detected, so this points to a normal condition of the transformer [71].

Contacting faults: Faults with contacts lead to increased resistance due to reduced conductivity. Cause for this can be lost terminal screws/clamps, corrosions, etc. The increased resistance causes a higher power loss when the current goes over the contact. The resulting increase in temperature can be detected with thermography. By evaluating thermo-images of the electrical contact or switch in scope at a certain current load, either compared to other components of the same type or compared to stored images of former thermo graphical investigations can be used to detect an increasing contact resistance [71].

Switching gear: The contact plates of switches will be eroded by sparks during each switching action. This causes burning marks on switch contacts and leads to an increased resistance. It will cause a higher contact temperature at the same current and there fore can be detected with thermography [71].

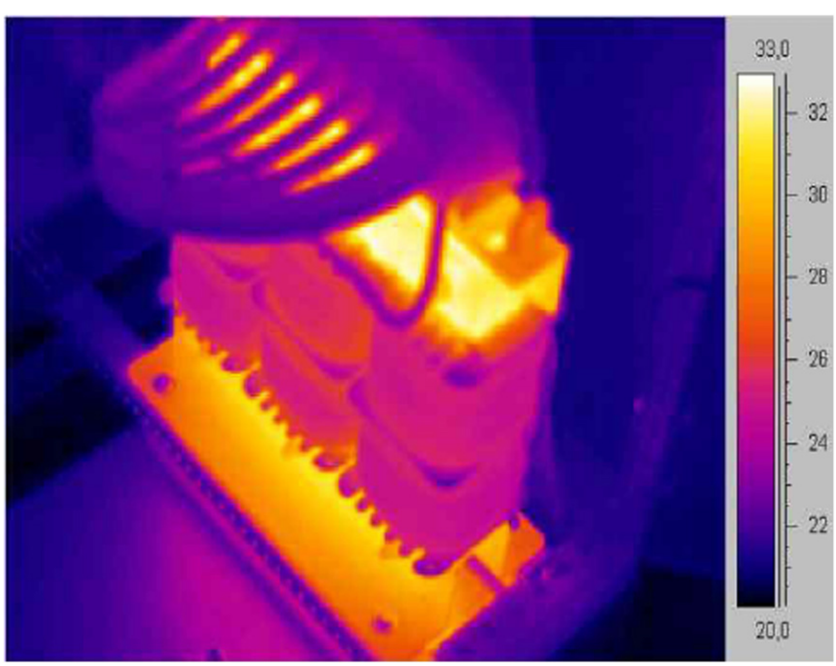


Fig. 58. Thermo image of a 3-phase transformer.

4. Conclusions and future works

CMS and FDS concepts presented in this paper can be applied to WEC to monitor, distinguish and detect, incipient faults in the main components. Implementation of these techniques entail initial investment but these costs are being offset by the benefits which are being reaped in the form of continuous production, minimum downtimes and more time available for an early planning to replace the defected parts. So, implementation of CMS and FDS are beneficial and can increase the profit margins substantially.

Future works include investigating in detail the further techniques on the basis of which novel and innovative CMS and FDS could be built.

Acknowledgment

This work was supported by the Korea Research Foundation Grant Funded by the Korea Government (MOEHRD) (KRF-2006-211-D00178).

References

[1] Joselin Herbert GM, Iniyan S, Sreevalsan E, Rajapandian S. A review of wind energy technologies. Renew Sustain Energy Rev 2007;11(6):1117–45.
[2] Fung KT, Scheffler RL, Stolpe J. Wind energy—a utility perspective. IEEE Trans Power Apparatus System 1981;100:1176–82.
[3] Ezio S, Claudio C. Exploitation of wind as an energy source to meet the world's electricity demand. Wind Eng 1998;74–76:375–87.
[4] Caselitz P, Giebhardt J. Advance maintenance and repair for offshore wind farms using fault prediction techniques. Institut fur Solare Energieversorgungstechnik (ISET), Division of Energy Conversion and Control Engineering Konigstor 59, D-34119 Kassel, Germany.
[5] Neumann D. Fault diagnosis of machine-tools by estimation of signal spectra. In: Proceedings of SAFEPROCESS'91, vol. I, 1991, Baden-Baden, p. 73–8.
[6] Schneider H, Frank PM. Observer-based supervision and fault detection for robots. In: Proceedings of TOOLDIAG'93, Toulous, 1993, p. 773–9.
[7] Caselitz P, Giebhardt J, Mevenkamp M. On-line fault detection and prediction in wind energy converters. Institut fur Solare Energieversorgungstechnik (ISET) e.V., Germany.
[8] ISET. Projeckgruppe Windenergie,WMEP Jahresauswer-tung 1992 und WMEP Jahresauswertung 1993, ISET e.V., Kassel.
[9] Ribrant J. Reliability performance and maintenance—a survey of failures in wind power systems. Master thesis, KTH School of Electrical Engineering, Sweden, 2005/2006.
[10] Chandler H, editor. Wind energy—the facts. European Wind Energy Association, 2003. Available at: 〈www.ewea.org06-05-02〉.
[12] Elforsk informerar. Vindkraft 2/05 Drift och underhåll av vindkraftverk. Elforsk, 2005. Available at: 〈www.vindenergi.org,06-05-02〉.
[13] Jonasson K. Tillståndsövervakning av vindkraftverk—Utvärdering av system utfört av SKF Nova, Elforsk rapport 01:30, 2001. Available at: 〈www.elforsk.se〉.
[14] Hansen TK. Project Team Manager, Elsam Engineering Denmark Interview with Johan Ribant [Ribrant J. Reliability performance and maintenance—a survey of failures in wind power systems. Master thesis, KTH School of Electrical Engineering, Sweden, 2005/2006], January 2006.
[15] Rao BKN, editor. Handbook of condition monitoring. Oxford: Elsevier Science Ltd; 1996, ISBN 1-85617-234-1.
[16] Verhoef JP, Verbruggen TW. Conditiebewaking aan windturbines; Een verkennende studie. ECN-C-058, Juni 2001.
[17] Verbruggen TW. Wind turbine operation & maintenance based on condition monitoring WT-Ω. Final report, ECN-C–03-047, April 2003.
[18] Knud Ole Helgesen Pedersen, Henrik Havemann. An Alternative approach to power engineering. Power Engineering Society Summer Meeting, 2000. IEEE 2000;4:2085–90. doi:10.1109/PESS.2000.866968.
[19] Walford CA. Wind turbine reliability: understanding and minimizing wind turbine operation and maintenance costs. Sandia Report, SAND2006-1100. Sandia National Laboratories, Albuquerque, New Mexico 87185 and Livermore, California 94550; 2006.
[20] Caselitz P, Giebhardt J. Rotor condition monitoring for improved operational safety of offshore wind energy converters. J Solar Energy Eng 2005;127:253.
[21] 〈www.smartfibres.com/SHM〉.
[22] 〈www.sensornet.co.uk〉.
[23] Wernicke J, Shadden J, Kuhnt S, Byars R, Rhead P, Damaschke. Field experience of fibre optical strain sensors for providing real time load information from wind turbine blades during operation. In: Paper presented at the European wind energy conference, London, UK, 2004, 22–25 November.
[24] Rao YJ. In-fibre Bragg grating sensors. Meas Sci Technol 1997; 8:355–75.
[25] Othonos A, Kalli K. Fibre Bragg gratings, 8 fundamentals and application in telecommunication and sensing. Boston, MA: Artech House; 1999.
[26] Ecke W, Latka I, Willsch R, Reutlinger A, Graue R. Fibre optic sensor network for spacecraft health monitoring. Meas Sci Technol 2001;12:974–80.
[27] Schroeder K, Ecke W, Apitz J, Lembke E, Lenschow G. A fibre Bragg grating sensor system monitors operational load in a wind turbine rotor blade. Meas Sci Technol 2006;17:1167–72.
[28] Lading L, McGugan M, Sendrup P, Rheinländer J, Rusborg J. Fundamentals for remote structural health monitoring of wind turbine blades—a preproject. Roskilde, Denmark: Risø National Laboratory; 2002.
[29] Jeffries WQ, Chambers JA, Infield DG. Experience with bicoherence of electrical power for condition monitoring of wind turbine blades. IEE Proc—Vis Image Signal Process 1998;145(3): June.
[30] Nikias CL, Mendel JM. Signal processing with higher order spectra. IEEE Signal Process Mag 1993:10–37.
[31] Hinich MJ, Clay CS. The application of the discrete Fourier transform in the estimation of power spectra, coherence and bispectra of geophysical data. Rev Geophys 1968;6(3):347–63.
[32] Swami A, Mendel JM, Nikias CL. Higher-order soectral analvsis toolbox. Natick, MA: The Math Works Inc.; 1995.
[33] Kim YC, Powers EJ. Digital bispectral analysis and its applications to nonlinear wave interactions. IEEE Trans Plasma Sci 1979;PS-7(2):120–31.
[34] Fackrell JWA, White PR, Hammond JK, Pnington RJ, Parsons AT. Bispectral analysis of periodic signals in noise: theory, interpretation and condition monitoring applications. In: Proceedings of signal processing, VII: theory and applications. European Association for Signal Processing; 1994. p. 1121–4.
[35] Dutton AG, Blanch MJ, Vionis P, Lekou D, van Delft DRV, Joosse PA, et al. Acoustic emission condition monitoring of wind turbine rotor blades:laboratory certification testing to large scale in-service deployment. Proceedings of the 2001 European wind energy conference, 2–6 July 2001, Copenhagen, Denmark.
[36] Schulz MJ, Sundaresan MJ. Smart sensor system for structural condition monitoring of wind turbines. Subcontract Report, NREL/SR-500-40089, August 2006. National Renewable Energy Laboratory, 1617 Cole Boulevard, Golden, Colorado 80401-3393, USA 〈www.nrel.gov〉.
[37] Sundaresan M, Grandhi G, Schulz M, Kirikera G. Embedded continuous sensor for monitoring damage evolution in composite

materials. In: SPIE conference on smart structures, devices, and systems, RMIT University, Melbourne, Australia, December 16–18, 2002.
[38] Caselitz P, Giebhargt J, Kruger T, Mevenkamp M. Development of a fault detection system for wind energy converters. Proceedings of the EUWEC '96, Gotegorg; 1996. p.1004–7.
[39] Caselitz P, Giebhargt J. Advanced condition monitoring system for wind engergy converters. Institut für Solare Energieversorgungstechnik e.V. Königstor 59, Kassel, Germany; 1999.
[40] Caselitz P, Giebhardt J, Mevenkamp M. Application of condition monitoring systems in wind turbine converters. Dublin: EWEC; 1997.
[41] Giebhardt J, Caselitz P, ISET; Rouvillain J, MITA Teknik DK; Lyrner T, Nordic Windpower, Sweden; C. Bussler, Plambeck Neue Energien; S. Gutt, Brüel & Kjaer Vibro; H. Hinrichs, Overspeed; Gram-Hansen K, Gram & Juhl, DK; Wolter N, Deutsche Montan Technologie; Giebel G, Risø, DK. Predictive. Condition monitoring for offshore wind energy converters with respect to the IEC61400-25standard. DEWEK, Wilhelmshaven, Germany, 2004. Available at: 〈www.iset.uni-kassel.de/osmr/〉.
[43] Popa LM, Jensen B-B, Ritchie E, Oldea I. Condition monitoring of wind generators. Industry applications conference, 2003. 38th IAS annual meeting. Conference record of the volume 3, 12–16 October 2003. p. 1839–46 (IEEE, CNF).
[44] Holst-Jensen O, Aarhus I. Advanced condition monitoring of wind turbines. The conference on "The Vibration Day 2001" organised by SVIB at the Royal Library in Copenhagen 21st November, 2001.
[45] Drouilhet S, Shirazi M. Wales, Alaska high-penetration wind–diesel hybrid power system theory of operation, Technical Report.
[46] Filbert D. Fault diagnosis in nonlinear electromechanical systems by continuous parameter estimation. ISA Trans 1985;24(3):23–7.
[47] Isemann R. Process fault detection based on modeling and estimation methods—a survey. Automatica 1984;20(4):387–404.
[48] Frank PM. Advances in observer-based fault diagnosis. In: Procedings of TOOLDIAG'93, Toulous, 1993, p. 817–36.
[49] Patton RJ, Frank PM, Clark RN, editors. Fault diagnosis in dynamic systems, theory and application. Englewood Cliffs, NJ: Prentice-Hall; 1989.
[50] Pau LF. Failure diagnosis and performance monitoring. New York: Marcel Dekker; 1981.
[51] Sturm A, Billardt S. Envelope curve analysis of machine with rolling-element bearings. In: Proceedings of SAFEPROCESS'91, vol. 2, Baden-Baden, 1991, p. 275–9.
[52] Frank PM. Diagnoseverfahren in der Automatisierungs-technik. Automatisierungstechnik 1994;42(2):47–64.
[53] Sora T, Koivo HN. Application of artificial neural networks in process fault diagnosis. In: Proceedings of SAFEPROCESS'91, vol. 2, Baden-Baden, 1991, p. 133–8.
[54] Tzafestas S. Second generation diagnostic expert systems: requirements, architectures and prospects. In: Proceedings of SAFEPROCESS'91, vol. 2, Baden-Baden, 1991, p. 1–6.
[55] Gentil S, Montmain J, Combastel C. Combining FDI and AI approaches within causal-model-based diagnosis. IEEE Trans Systems Man Cybernet—Part B: Cybernet 2004;34(5):1.
[56] Poole D. Normality and faults in logic-based diagnosis. In: Proceedings of the international joint conference on artificial intelligence, 1989, p. 1304–10.
[57] Struss P. AI methods for model-based diagnosis. In: Twelfth international workshop principles diagnosis DX01-bridge workshop, Via Lattea, Italy, 2001.
[58] Reiter R. A theory of diagnosis from first principles. Artif Intell 1987;2:57–95.
[59] Dague P, Dubuisson B. Diagnostic par intelligence artificielle et reconnaissance des formes. Paris, France: Hermès; 2001.
[60] Ligeza A, Górny B. Systematic conflict generation in model based diagnosis. In: Proceedings of the IFAC safeprocess on fault detection. Supervision and safety for technical processes, 2000, p. 1103–8.
[61] Darwiche A. Model-based diagnosis using structured system descriptions. J Artif Intel Res 1998;8:165–222.
[62] Frank P. Analytical and qualitative model-based fault diagnosis, a survey and some new results. Eur J Control 1996;1(2):6–28.
[63] Frank P, Ding S. Current development in the theory of FDI. In: Proceedings of the IFAC safeprocess on fault detection. Supervision and safety for technical processes, 2000, p. 16–27.
[64] Ghoshal A, Sundaresan MJ, Schulz MJ, Paib PF. Structural health monitoring techniques for wind turbine blades. J Wind Eng Ind Aerodynam 2000;85:309–24.
[65] Sundaresan MJ, Schulz MJ, Ghoshal A. Structural health monitoring static test of a wind turbine blade. NREL Subcontract Report No.: NREL/SR-500-28719, March 2002. National Renewable Energy Laboratory, 1617 Cole Boulevard, Golden, Colorado 80401-3393, USA.
[66] Dutton AG. Thermoelastic stress measurement and acoustic emission monitoring in wind turbine blade testing. 2004 European Wind Energy, Conference & Exhibition 22–25 November, 2004; London, UK.
[67] IEC 61400-1, Wind turbine generator systems-part 1: safety requirements. 2nd ed., 1998.
[68] Paynter RJH, Dutton AG. The use of a second harmonic correlation to detect damage in composite structures using thermoelastic stress measurements. Strain 2003;39:73–8.
[69] Garcia MC, Sanz-Bobi MA, del Pico J. SIMAP: intelligent system for predictive maintenance application to the health condition monitoring of a windturbine gearbox. J Comput Ind 2006;57(6):552–68.
[70] Development of prognostic/health management (PHM) technologies for wind turbines: final report. Prepared by: Dr. Neil Baines and Dr. Tim Way, 2006.
[71] Final Report: advanced maintenance and repair for offshore wind farms using fault prediction and condition monitoring techniques (Offshore M&R), funded by the European Commission, DG TREN under the FP5 Contract NNE5/2002/710, Duration 2003-01-01 to 2005-12-31.
[72] Dunkers JP. Applications of optical coherence tomography to the study of polymer matrix composites. In: Bouma B, Tearney G, editors. Handbook of optical coherence tomography. Marcel Dekkar, Inc.; 2002.